DISSERTATIONES
TECHNOLOGIAE
CIRCUMIECTORUM
UNIVERSITATIS
TARTUENSIS
43

KAIRI ADAMSON

Applicability of digital photography in monitoring changes of leaf inclination and foliage clumping with time

DISSERTATIONES TECHNOLOGIAE CIRCUMIECTORUM
UNIVERSITATIS TARTUENSIS
43

DISSERTATIONES TECHNOLOGIAE CIRCUMIECTORUM
UNIVERSITATIS TARTUENSIS
43

KAIRI ADAMSON

Applicability of digital photography in monitoring changes of leaf inclination and foliage clumping with time

UNIVERSITY OF TARTU
Press
1632

Department of Remote Sensing, Tartu Observatory, Faculty of Science and Technology, University of Tartu, Estonia.

Dissertation was accepted for the commencement of the degree of *Doctor philosophiae* in Environmental Technology at the University of Tartu on the 14th of August 2024 by the Scientific Council on Environmental Technology, University of Tartu.

Supervisor:	Associate Professor Jan Pisek, Tartu Observatory, University of Tartu, Estonia
Opponent:	Dr. Loïc Tadrist, Aix-Marseille Université, France
Commencement:	Oecologicum (J. Liivi 2, Tartu), room 127, on the 24th of September 2024 at 14:15.

Publication of this thesis is granted by the Tartu Observatory, University of Tartu.

ISSN 1736-3349 (print)
ISBN 978-9916-27-633-4 (print)
ISSN 2806-2612 (pdf)
ISBN 978-9916-27-634-1 (pdf)

University of Tartu Press
www.tyk.ee

CONTENTS

LIST OF ORIGINAL PUBLICATIONS

This thesis is based on the following publications, which are referred to in the text by their Roman numerals. The full texts are included at the end of the thesis.

I **Raabe, K.**, Pisek, J., Sonnentag, O., Annuk, K. (2015). Variations of leaf inclination angle distribution with height over the growing season and light exposure for eight broadleaf tree species. Agricultural and Forest Meteorology, 214–215, 2–11. https://doi.org/10.1016/j.agrformet.2015.07.088.

II **Raabe, K**., Pisek, J., Lang, M., Korhonen, L. (2017). Estimating the beyond-shoot foliage clumping at two contrasting points in the growing season using a variety of field-based methods. Trees, 31, 1367–1373. https://doi.org/10.1007/s00468-017-1541-7.

III Pisek, J., Řezníčková, L., **Adamson, K.**, Ellsworth, D.S. (2021). Leaf inclination angle and foliage clumping in an evergreen broadleaf Eucalyptus forest under elevated atmospheric CO_2. Australian Journal of Botany, 69 (8), 622–629. https://doi.org/10.1071/BT21035.

IV Chianucci, F., Pisek, J., **Raabe, K.**, Marchino, L., Ferrara, C., Corona, P. (2018). A dataset of leaf inclination angles for temperate and boreal broadleaf woody species. Annals of Forest Science, 75, 50. https://doi.org/10.1007/s13595-018-0730-x.

V Pisek, J., **Adamson, K.** (2020). Dataset of leaf inclination angles for 71 different Eucalyptus species. Data in Brief, 33, 106391. https://doi.org/10.1016/j.dib.2020.106391.

Author's contribution

The articles on which this thesis is based are the result of collective work. The author's contribution to the publications is denoted as: '*' a minor contribution, '**' a moderate contribution, '***' a major contribution.

Categories	Author's contribution				
	I	II	III	IV	V
Original idea	***	**	*	*	*
Study design	***	***	*	*	*
Data processing and analysis	***	***	**	**	**
Interpretation of the results	***	***	**	*	*
Writing the manuscript	***	***	*	*	*

Other related publications of the dissertant. The texts are not included as full texts at the end of the thesis.

1. Kattge, J., Boenisch, G., Diaz, S., Lavorel, S., Prentice, I.C., Leadley, P., Tautenhahn, S., Werner, G.D.A., Aakala, T., Abedi, M., Acosta, A.T.R., Adamidis, G.C., **Adamson, K.**, Aiba, M., Albert, C.H., Alcantara, J.M., Alcazar, C.C., Aleixo, I., Ali, H., Amiaud, B., …, Wirth, C. (2020). TRY plant trait database – enhanced coverage and open access. Global Change Biology, 26 (1), 119–188. https://doi.org/10.1111/gcb.14904.
2. Moser, W.K., Coble, A.P., Hallik, L., Richardson, A.D., Pisek, J., **Adamson, K.**, Graham, R.T., Moser, C.F. (2020). Advances in understanding canopy development in forest trees. In: Stanturf, J. (Ed.). Achieving sustainable management of boreal and temperate forests (59–98). Sawston Cambridge, UK: Burgleigh Dodds Science Publishing Limited. (Burleigh Dodds Series in Agricultural Science). https://doi.org/10.19103/AS.2019.0057.04.
3. Meerdink, S., Roberts, D., Hulley, G., Gader, P., Pisek, J., **Adamson. K.**, King, J., Hook, S.J. (2019). Plant species' spectral emissivity and temperature using the hyperspectral thermal emission spectrometer (HyTES) sensor. Remote Sensing of Environment, 224, 421–435. https://doi.org/10.1016/j.rse.2019.02.009.

ABBREVIATIONS

DCP – digital cover photography
DHP – digital hemispherical photography
EucFACE – Eucalyptus free-air CO_2 enrichment
LAI – leaf area index
LAI_e – effective leaf area index
LIA – leaf inclination angle
LIAD – leaf inclination angle distribution
LiDAR – light detection and ranging
MISR – Multi-angle Imaging SpectroRadiometer
MODIS – Moderate-resolution Imaging Spectroradiometer
NDHD – normalized difference between hotspot and darkspot
P – gap fraction
POLDER – Polarization and Directionality of the Earth's Reflectances
RAMI – Radiation Model Intercomparison
TLS – terrestrial laser scanning
TRAC – Tracing Radiation and Architecture of Canopies
Ω – foliage clumping

1. INTRODUCTION

1.1 Background

Light is a highly heterogeneous environmental factor, playing a crucial role in regulating plant growth, survival, and competitive dynamics within ecosystems (Canham et al., 1990). Close to linear positive relationships have been observed between the amount of intercepted light and canopy productivity, demonstrating that light interception by canopies is a vital ecosystem-scale driver of productivity (Duursmaa and Mäkelä, 2007; Niinemets, 2010).

Effective light capture is particularly important for plants growing in competition within dense vegetation (Valladares and Niinemets, 2008). Plants have the potential to enhance overall canopy light interception, for example by increasing either the total leaf area or the efficiency of each unit of leaf area in capturing light (Niinemets and Fleck, 2002). However, there are inherent genetic and mechanical constraints limiting the maximum efficiency of light capture, such as leaf structure, maximum attainable plant height, and the biomass required for optimal leaf exposure. For example, the biomass costs associated with leaf exposure escalate as leaves are positioned farther apart and higher up the stem. Consequently, plants are unable to fully expose all their foliage to direct sunlight (Niinemets, 2010). Given these limitations, adjustments in leaf inclination angles offer a significant means to alter the foliage's capacity for light interception (Niinemets and Fleck, 2002).

Leaf inclination angle (LIA) is the angle between the leaf normal and the zenith, or between the leaf plane and horizontal plane (Yang et al., 2023). It is a crucial leaf characteristic linked to light interception, photosynthesis, energy balance, and competition among individual plants (Anten, 2005; Nilsen and Forseth, 2018). These effects of LIA can scale up to substantially influence land surface properties, including carbon flux and spectral signature (Baldocchi et al., 2002; Ollinger, 2011). Despite the importance of leaf inclination angle being recognized in quite early ecological studies (Yin, 1938; Monsi and Saeki, 1953), it remains frequently underrepresented in models and seldom measured in the field.

Leaf inclination angle distribution (LIAD), the statistical distribution of the fraction of leaf area at any given leaf inclination angle, is generally used to describe the leaf inclinations within a canopy (Yang et al., 2023). For simplicity, the LIADs are often fitted into six commonly used classical types, which offer easier interpretations compared to the parameter values of statistical distributions. These LIAD types include planophile, plagiophile, uniform, spherical, erectophile and extremophile (de Wit, 1965; Fig. 1). For canopies with a spherical LIAD, the relative frequency of leaf inclination angles is the same as the relative frequency of the inclinations of the surface elements of a sphere; for uniform canopies, the proportion of leaf inclination angles is the same at any angle; planophile canopies are dominated by horizontal or close to horizontal leaves; plagiophile canopies

are dominated by inclined leaves, and extremophile canopies by high frequencies of both horizontally and vertically oriented leaves (Lemeur and Blad, 1974).

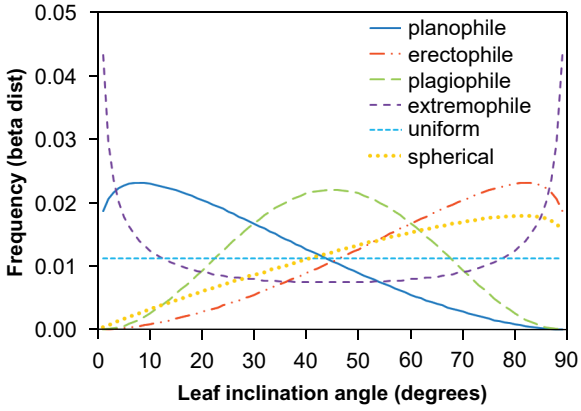

Figure 1. Beta distributions for the six theoretical leaf inclination angle distributions. Adopted from Article ***I****.*

Another widely used option for the description of leaf inclination angle distributions is the G-function. G-function is the ratio of the leaf area projected on the plane perpendicular to the incoming solar beam and the actual leaf area (Ross, 1981). It is a vital canopy structural parameter widely used in radiative transfer modelling, and along with the clumping index (Ω) and leaf area index (LAI), it allows for the estimation of the gap fraction of a canopy. Gap fraction, in turn, is defined as the portion of the sky that is visible through the canopy (Welles and Norman, 1991).

For the entire canopy, the probability of light transmission, i.e. gap fraction, at an angle θ through a canopy can be expressed using Beer's law (Monsi and Saeki, 1953, 2005) as follows:

$$P(\theta) = exp\left[\frac{-G(\theta)LAI\Omega}{\cos\theta}\right]. \quad (1)$$

Here, P denotes the probability of a gap, G is the G-function, LAI stands for leaf area index, Ω represents the clumping index, and θ is the view zenith angle. Thus, three crucial parameters of canopy structure are generally necessary to comprehensively describe light penetration within a canopy: the amount of leaves (LAI), the orientation of the leaves (LIAD), and their spatial distribution (the clumping index).

The canopy clumping index quantifies foliage's distribution in space and is another significant factor influencing light distribution within a canopy (Nilson, 1999; Valladares and Guzman, 2006). It is defined as the ratio of the effective leaf area index to the true leaf area index (Nilson, 1971; Fang, 2021):

$$\Omega \equiv LAI_e/LAI \quad (2)$$

LAI describes the total one-sided area of all green leaves in the canopy per unit ground surface and is identified as an essential climate variable by the Global Climate Observing System (GCOS, 2016). It is likely the most extensively studied canopy structure parameter. Effective LAI (LAI_e) is the LAI value that would produce the same indirect gap fraction measurement as that observed, assuming a simple random foliage distribution (Chen et al., 2005). To correctly estimate LAI using the indirect optical approach based on measuring LAI_e, accurate knowledge of the clumping index is essential. By enhancing the separation of sunlit and shaded leaves, clumping also profoundly effects the radiation regime of a plant canopy and photosynthesis (Oker-Blom et al., 1983; Davi et al., 2006).

The clumping of canopy elements takes place hierarchically in all types of forests, progressing from rosettes of leaves and shoots to crowns, individual trees, clusters of trees and finally to forest patches (Fournier et al., 1997). The value of the clumping index Ω describes the organization in canopies, with $\Omega = 1$ indicating a random foliage distribution, $\Omega > 1$ for regularly distributed foliage elements, and $\Omega < 1$ where the foliage elements are clumped. Theoretically, the clumping index value can range from zero (all foliage elements stacked on top of each other) to infinity (all foliage elements arranged side by side). In practice, it has been shown that generally Ω varies between 0.3 for highly clumped canopies to 1.0 for randomly distributed foliage (Wei et al., 2019).

Prior to the clumping index, a foliage dispersion parameter was often calculated from a contact number using the relative variance approach (Warren Wilson, 1965; Myneni et al., 1989). A significant distinction between this foliage dispersion parameter and the clumping index is in their quantifications: the former is based on the ratio of canopy gap fractions under actual versus random conditions, while the latter quantifies the ratio between LAI_e and LAI (Fang et al., 2021). The clumping index also differs from the aggregation metrics used in landscape ecology and spatial statistics, which, though conceptually similar, cannot be applied in land surface models. In landscape ecology, aggregation and clumpiness indices are calculated as a measure of spatial aggregation on a landscape unit level (Rasmussen et al., 2011); spatial statistics provide tools to analyze the non-randomness patterns of spatial points (Perry et al., 2016). Neither equals to the clumping index, which is specifically defined for the non-randomness of the distribution of individual leaves or needles and thus suited to quantify the transmittance and interception of light and precipitation (Fang et al., 2021).

1.1.1 Leaf inclination angle measurements and applications

Measuring leaf inclination angles has generally been a difficult task, particularly in complex canopies, and as a result, it has often been inadequately represented in models. The methods used for LIA measurements have ranged from labor-intensive manual methods to the application of advanced and costly instruments.

The simplest and most tedious method has been measuring the leaf inclination angles by hand, using a compass-protractor (Laisk, 1965; Norman and Campbell, 1989) or an inclinometer. Both allow measuring the LIA as well as the leaf

azimuth. A more elaborate instrument for direct LIA measurements was devised by Lang (1973). Called the Spatial Coordinate Apparatus, it measures the coordinates of the apices of triangles, into which the surface of the leaf is divided. Selecting multiple triangles, the position, inclination angle and azimuth angle of the leaf can be measured. A more modern version of this method is a 3D digitizer (Falster and Westoby, 2003) consisting of a magnetic signal receiver and pointer, which allows recording spatial coordinates of the pointer in a specific range of the receiver. Sinoquet et al. (2009) used a similar device with a pointer in an electromagnetic field to record 3D maps of leaf geometry.

The inclined-point-quadrat method (Warren Wilson, 1960) is based on inserting a probe with a sharp tip into the canopy at a known inclination and azimuth angle and counting the number of times the point contacts leaves. The average leaf angle can be estimated based on the number of contacts at multiple inclination angles. This method addressed the difficulty of measuring the LIA of needleleaf species compared to broadleaves, but nowadays the method is becoming more of a predecessor to more rapid indirect methods. All the previously described methods are very time-consuming, limited by canopy height and foliage movements due to wind, and unrealistic to use if the goal is to obtain a full leaf inclination angle distribution of a canopy.

A series of faster, less labor-intensive methods are based on using upward hemispherical photography (Lerdau et al., 1992), a plant canopy analyzer (Welles and Norman, 1991) or leveled digital photography (Ryu et al., 2010a). The first two of these approaches estimate the G-function at various viewing angles and derive the mean leaf inclination angle, assuming all leaves on a canopy are oriented at the same zenith angle and have a uniform azimuthal angle distribution. The leveled digital camera method (detailed in section 2.2.1) is based on measuring LIA manually from photos taken by a horizontally mounted camera using image processing software. Although relatively time-consuming, the approach is cheap and simple, requiring very little training and readily available equipment.

The most sophisticated methods so far are based on terrestrial laser scanning (TLS). TLS instruments are ground-based devices using light detection and ranging (LiDAR) to hemispherically measure distances with very high resolution, enabling automatically measuring leaf inclination angles (Stovall et al., 2021). Undergone significant advances in the last decade (Hosoi and Omasa, 2009; Lau et al., 2019; Disney et al., 2019), TLS has become the most cutting-edge instrument for capturing canopy structure in three dimensions. The data acquisition with LiDAR is rapid, robust, and repeatable, providing the most detailed leaf inclination angle information compared to methods that subsample a small set of leaves (Yang et al., 2023). However, disadvantages arise from the high costs, occlusion effects, time-consuming post processing as well as the extensive expert knowledge required to process the data. Additionally, there can be problems with leaf area weighting, as TLS-based estimates are biased toward leaves with a normal parallel to the laser direction and tend to underestimate the proportion of planophile leaves (Bailey and Mahaffee, 2017).

Correct leaf inclination angle data is crucial for accurate modeling of radiative transfer, light interception, and leaf energy balance. Despite this, LIAD has often been fully neglected in land surface models (Smith, 2001; Sato et al., 2007) or assumed to be spherical for all canopies (Pinty et al., 2006; Farrior et al., 2013). In other models it has been considered at plant functional type level and treated as fixed during the growing season (Wang and Leung, 1998; Lawrence et al., 2019; Koven et al., 2020). More detailed leaf inclination angle data has been used in models which instead of global calculations focus on a small set of individuals (Pearcy and Yang, 1996; Gastellu-Etchegorry et al., 2017).

Leaf inclination angle is a highly influential parameter in the simulation of optical signals as well as carbon, water, and energy fluxes. It significantly impacts canopy radiative transfer and directly affects the modeling of carbon and water fluxes by controlling the surface area available to intercept and scatter sunlight (Yang et al., 2023). Simulations from a radiative transfer model have shown that variations in LIAD can lead to changes as substantial as a four-fold difference in net carbon uptake rates and approximately 20% in both sensible and latent heat fluxes (Baldocchi et al., 2002). LIA also has an indirect impact on the aforementioned processes by affecting the estimation of LAI, which can differ by ~25% between cases where accurate LIA measurements are used or not (Stovall et al., 2021).

Currently, no well-known land surface model considers the vertical distribution of leaf inclination angles (Bonan et al., 2021). Considering the importance of LIA, including data on the seasonal and vertical variations in leaf inclination angle could have a significant impact on the modelling of canopy photosynthesis (Stovall et al., 2021).

1.1.2 Clumping index measurements and applications

Various methods have been used to estimate the clumping index. These methods can generally be categorized as direct methods, where effective LAI is divided by true LAI; indirect optical methods, based on LAI_e or the distribution of gaps; allometric methods utilizing the relationship between foliage clumping and other structural variables; and proxy methods, which describe the spatial distribution patterns of leaves in a related but different way (Fang et al., 2021).

In the field, several optical instruments have been used for LAI_e measurements and clumping index estimations. These include digital cover photography (DCP) (Chianucci et al., 2016), digital hemispherical photography (DHP) (Leblanc et al., 2005a), the LAI-2000 or LAI-2200 plant canopy analyzer (Welles and Norman, 1991) and the tracing radiation and architecture of canopies (TRAC) instrument (Chen and Cihlar, 1995). In the case of direct clumping index estimates, the LAI_e acquired by aforementioned instruments is divided by true LAI obtained by measuring the area of leaf samples or leaf litters (Baret et al., 2010; Nasahara et al., 2008). For indirect clumping index estimation, the data from these instruments is used to estimate clumping index by calculating canopy gap fractions (Fang et al., 2021).

Indirect optical methods for clumping index measurement are non-destructive and cost-effective but each have their limitations. For example, the accuracy of clumping index estimation from DHP is dependent on the accuracy of the classification of plant pixels and gaps from the photos. Theoretically the entire 0–90° view angle is required to estimate Ω, but it is rarely utilized due to higher classification uncertainties for large zenith angles (Jonckheere et al., 2004). LAI-2200 calculates the ratio between the above- and below-canopy radiation as the canopy gap fraction for five concentric conical rings centered at 7°, 23°, 38°, 53°, and 68° (LI-COR, 2010). The outer rings are often affected by diffuse light from multiple scattering and the data used may be limited to the inner rings (Chen, 1996; Stroppiana et al., 2006). TRAC instrument records the transmitted direct light along a transect and identifies canopy gaps from the measured sunlit segments along the transects at least ten times longer than the average tree spacing, essentially recording the sunlight transect length, but not the actual gaps or gap sizes (Chen and Cihlar, 1995). The method is influenced by the solar zenith angle, the limited field of view (Chen and Cihlar, 1995), and the gap threshold and gap removal processes (Zou et al., 2015).

At large spatial scales, clumping index is estimated from optical remote sensing data through an empirical relationship with vegetation indices or the normalized difference between hotspot and darkspot (NDHD) index (Chen et al., 2005; Leblanc et al., 2005b). Global clumping index products have been created first using POLDER data (Roujean and Lacaze, 2002) and due to POLDER's limited availability and low spatial resolution, later almost exclusively from the Moderate Resolution Imaging Spectroradiometer (MODIS) sensor (Hill et al., 2011; He et al., 2012; Wei et al., 2019). Multi-Angle Imaging Spectroradiometer (MISR) has also been used for clumping index estimation (Pisek et al., 2013b).

The most important application of the clumping index is in the transformation between effective LAI and true LAI (Fang et a., 2021). Allowing for better separation of sunlit and shaded leaves, it is also utilized in canopy reflectance models (e.g. Kuusk, 2001; Pinty et al., 2006; Ni-Meister et al., 2010) as well as land surface models (e.g. Chen et al., 2012; Lunka and Patil, 2016; Brahgiere et al., 2020). With growing availability of field measurements and remote sensing data, the clumping effect can be represented in models with increased accuracy.

1.2 Motivation and objectives

This study was primarily motivated by the infrequent incorporation of the crucial leaf inclination and clumping data in modeling. The aim was to test and compare LIA and clumping index measurement methods, with a focus on accessible digital photography based methods, to explore the complexity of both parameters, and to provide usable datasets for modeling.

The main objectives of this study were:

- to establish the robustness of the digital camera method for measuring leaf inclination (**I**);
- to evaluate digital photography based approaches for clumping index estimation compared to alternative, previously used instruments and methods (**II**);
- to examine how the leaf inclination angle distribution and foliage clumping may vary with season, height in the canopy, light exposure, and the expected elevated atmospheric CO_2 concentrations in the future (**I**, **II**, **III**).

To achieve the objectives, the following hypotheses were proposed:

- the leveled digital photography method is a robust means for measuring leaf inclination angles that is insensitive to user's expertise;
- the leaf inclination angle is highly dependent on season, height in the canopy, and light exposure;
- digital photography-based methods provide a reliable, cost and labor-effective way to estimate clumping index;
- elevated atmospheric CO_2 levels do not significantly affect leaf inclination angle distribution and foliage clumping.

2. MATERIALS AND METHODS

2.1 Study sites

The study sites included in this thesis cover a wide geographical range and various vegetation types, from Estonian hemi-boreal forests to *Eucalyptus* stands in Australia (Fig. 2).

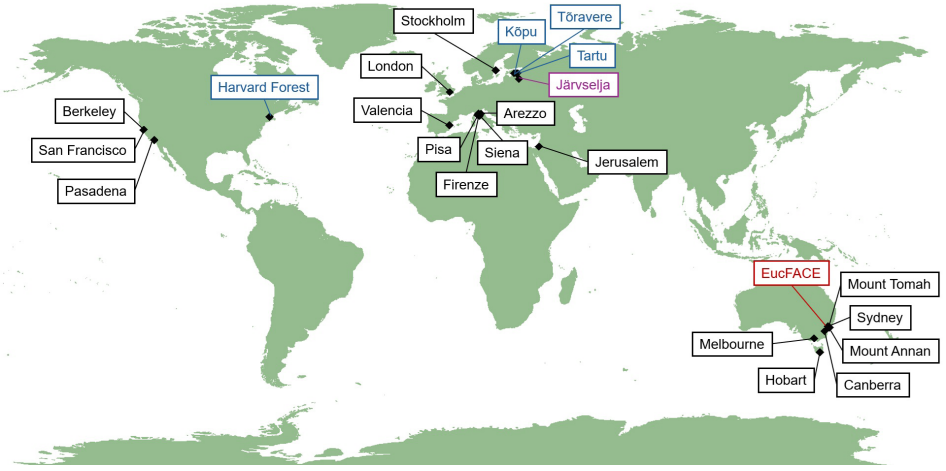

Figure 2. Locations of the study sites. Sites presented in blue were used in study ***I****, Järvselja (purple) was used in studies* ***I*** *and* ***II****, and EucFACE (red) was investigated in study* ***III****. All sites except EucFACE were included in the data presented in studies* ***IV*** *and* ***V****.*

Leaf inclination data for study **I** was gathered at five different sites in Estonia: Tartu Observatory, Tõravere (58.27°N; 26.46°E; referred to as Tõravere); Järvselja (56.27°N; 27.32°E); Tartu (58.38°N; 26.72°E); and Kõpu (58.33°N; 25.30°E). The measurements were done in open parks or plantations on stand-alone trees or small clusters of trees, except the forest site in Järvselja. Study **I** additionally contains data from Harvard Forest Environmental Measurement Site, Petersham, MA, USA (42.54°N; 72.17°W). The site, at the time of measurements, was a 50–70-year-old mixed-hardwood forest stand.

Two mature forest stands, included in the Radiation Model Intercomparison (RAMI) exercise (Widlowski et al., 2015) and located in Järvselja, Estonia, were investigated in study **II**. The first stand was a 54-year-old fertile Silver birch (*Betula pendula* Roth.) dominated area with an understory consisting of hazelnut (*Corylus avellana* L.) and small-leaved linden (*Tilia cordata* Mill.). The second stand was a 128-year-old Scots pine (*Pinus sylvestris* L.) forest growing on a transitional bog. Both stands encompass a sample plot measuring 100 × 100 m, where all optical measurements were conducted.

In study **III**, the measurements were carried out at the Eucalyptus free-air CO_2 enrichment (EucFACE) facility located in Cumberland Plain, western Sydney, Australia (33.62°S, 150.73°E). The vegetation in this area comprises an open woodland primarily dominated by a single species (*Eucalyptus tereticornis* Sm.) with a minor presence of *Eucalyptus amplifolia* Naudin. The understory consists mainly of grasses, along with lower densities of forbs and shrubs.

Studies **IV** and **V** present data largely obtained for stand-alone trees from botanical gardens in various locations with significantly different climatic conditions and vegetation types. These sites include the Bergius Botanical Garden, Stockholm, Sweden (59.37°N, 18.05°E); Australian National Botanic Gardens, Canberra, ACT, Australia (35.28°S, 149.11°E); Royal Botanic Gardens, Sydney, NSW, Australia (33.86°S, 151.22°E); Royal Tasmanian Botanical Gardens, Hobart, TAS, Australia (42.87°S, 147.33°E); The Jerusalem Botanical Gardens, Jerusalem, Israel (31.77°N, 35.2°E), Jardì Botànic de València, Spain (39.48°N, 0.39°W); Royal Botanic Gardens, Kew, the United Kingdom (51.48°N, 0.30°W); San Francisco Botanical Garden, San Francisco, CA, USA (37.77°N, 122.47°W); University of California Botanical Garden at Berkeley, Berkeley, CA, USA (37.87°N, 122.24°W), Monteverdi Marittimo, Pisa, Italy (43.21°N, 10.70°E); Firenze, Italy (43.77°N, 11.23°E), and others (full lists in articles **IV** and **V**).

2.2 Leaf inclination angles

2.2.1 Measurement methodology

The leaf inclination angles in studies **I**, **III**, **IV** and **V** were measured using the leveled digital photography method. Originally introduced by Ryu et al. (2010a) and later validated by Pisek et al. (2011a), this method involves capturing a series of leveled digital images of the tree crown under calm conditions to minimize the impact of wind on leaves (Tadrist et al., 2014). The images are then visually inspected to identify leaves whose surfaces are approximately perpendicular to the digital camera's viewing direction (Fig. 3). The inclination angles of these suitable leaves were measured using the public domain image processing software ImageJ (https://imagej.net/ij/; visited 25.07.24). While it has been suggested that measuring hundreds of leaves is necessary for an accurate representation of leaf inclination angles (Kucharik et al., 1998), Pisek et al. (2013a) demonstrated that around 75 leaves may be sufficient to obtain a representative distribution of leaf inclination angles. In this work, whenever possible, around 75–100 leaves were measured.

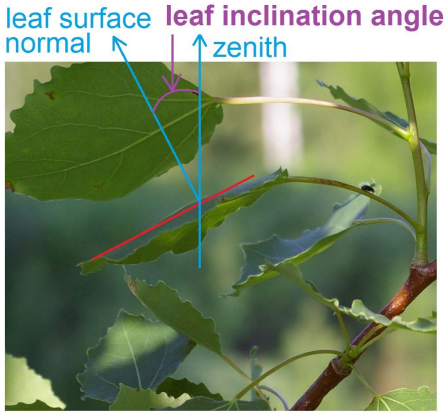

Figure 3. Photographic leaf inclination angle measurement with leaf surface normal oriented approximately perpendicular to the viewing direction of the digital camera. The red line is the geometrical representation of the leaf, from which the angle is measured. Adopted from Article ***I****.*

The leaf inclination angle distribution was estimated assuming a uniform distribution of leaf azimuth angle and leaf inclination angle being independent of leaf size. The two-parameter beta distribution (Goel and Strebel, 1984) has been previously evaluated as the most appropriate function to represent the probability density of θ_L (Wang et al., 2007):

$$f(t) = \frac{1}{B(\mu,\nu)}(1-t)^{\mu-1}t^{\nu-1} \tag{3}$$

where $t = 2\theta_L/\pi$. The beta-distribution function $B(\mu,\nu)$ is defined as

$$B(\mu,\nu) = \int_0^1 (1-x)^{\mu-1}x^{\nu-1}dx = \frac{\Gamma(\mu)\Gamma(\upsilon)}{\Gamma(\mu+\nu)} \tag{4}$$

with Γ for the Gamma function and μ and ν being two beta distribution parameters calculated as

$$\mu = (1-\bar{t})\left(\frac{\sigma_0^2}{\sigma_t^2} - 1\right) \tag{5}$$

$$\nu = \bar{t}\left(\frac{\sigma_0^2}{\sigma_t^2} - 1\right) \tag{6}$$

where σ_0^2 is the maximum standard deviation with expected mean $\bar{t}$ and σ_t^2 is variance of t (Wang et al., 2007).

Measured leaf inclination angle distributions were categorized by identifying the distribution type closest to them. To quantify each leaf inclination distribution's deviation from the distributions suggested by de Wit ($f_{\mathrm{deWit}}(\theta_L)$), a modified version of the inclination index by Ross (1975) was used:

$$\chi_L = \int_0^{\frac{\pi}{2}} |f(\theta_L) - f_{\mathrm{deWit}}(\theta_L)| d\theta_L \quad (7)$$

Additionally, the G-function values were calculated for each dataset. The value of the G-function can be calculated by integrating the leaf angle distribution function $f(\theta_L)$ over the leaf inclination angle θ_L. Assuming an azimuthally symmetric canopy, it can be written as:

$$G(\theta) = \int_0^{\frac{\pi}{2}} A(\theta, \theta_L) f(\theta_L) d\theta_L \quad (8)$$

Where A is the G-function for a canopy having all leaves inclined at θ_L and θ being the view zenith angle (Warren Wilson, 1960):

$$A(\theta, \theta_L) = \begin{cases} \cos\theta \cos\theta_L, & |\cot\theta \cot\theta_L| > 1 \\ \cos\theta \cos\theta_L \left[1 + \frac{2}{\pi}(\tan\psi - \psi)\right], & |\cot\theta \cot\theta_L| \leq 1 \end{cases} \quad (9)$$

$$\psi = \cos^{-1}(\cot\theta \cot\theta_L). \quad (10)$$

2.2.2 User subjectivity

In study **I**, the robustness of the leveled digital camera method was evaluated regarding its sensitivity to user subjectivity. For this purpose, ten users measured leaf inclination angles from the same four sets of images. The users had varying levels of previous experience, ranging from beginners with no prior knowledge of leaf inclination angles to experts well-versed in the method. The comparison of results included the mean leaf inclination angles, their standard deviations, and the resulting beta distributions.

2.2.3 Variability with season, height in the canopy, and light exposure

Vertical variations in leaf inclination angle distributions throughout the growing season were examined for five broadleaf species growing in open, well-lit environments (study **I**). Additionally, four broadleaf species were studied in natural forests to evaluate the impacts of varying light exposure. The images were captured at multiple height levels and categorized broadly into three canopy sections – bottom, middle, and top. The leaf inclination angles measured from each set were fitted with the beta distribution and matched with the closest de Wit (1965) theoretical leaf inclination angle distribution.

2.3 Foliage clumping

Four different optical means of data collection and six calculation methods for estimating foliage clumping (Ω) were used in study **II** (table 1). Data was obtained via digital hemispherical photography, digital cover photography, the TRAC instrument and LAI-2000 instrument.

Table 1. Overview of the calculation methods used with each instrument for clumping index estimation.

	DHP	**DCP**	**TRAC**	**LAI-2000**
Image of the instrument/ photography type	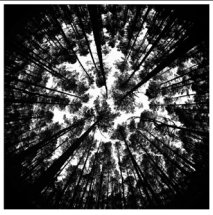			
Calculation methods	LX (Eq. 11) CC (Eq. 12) CLX (Eq. 13)	Macfarlane (Eq 14–15) Kucharik (Eq. 16–17)	LX (Eq. 11) CC (Eq. 12) CLX (Eq. 13)	Apparent clumping (Eq. 18)

2.3.1 Calculation methods

Clumping index from logarithmic average (LX)

In the finite-length (LX) method proposed by Lang and Xiang (1986), clumping is assessed for small segments with a length ideally ten times the width of foliage elements. The clumping index calculation utilizes the gap fraction, denoted as P in the view direction θ, and is expressed as follows:

$$\Omega_{LX}(\theta) = \frac{\ln[\overline{P(\theta)}]}{\overline{\ln[P(\theta)]}} \tag{11}$$

Here, $\overline{P(\theta)}$ represents the canopy's mean gap fraction, and $\overline{\ln[P(\theta)]}$ is the logarithmic mean derived from the gap fractions of all segments.

Clumping index from gap size distribution (CC)

Ω_{CC} is estimated after the method of Chen and Cihlar (1995), corrected by Leblanc (2002):

$$\Omega_{CC}(\theta) = \frac{\ln[F_m(0,\theta)][1-F_{mr}(0,\theta)]}{\ln[F_{mr}(0,\theta)][1-F_m(0,\theta)]} \tag{12}$$

The approach relies on categorizing gaps according to their sizes. $F_m(0,\theta)$ represents the total cumulative canopy gap fraction, while $F_{mr}(0,\theta)$ denotes the reduced cumulative gap-size fraction, excluding large, non-random gaps.

Clumping index from the combination of gap size and logarithm methods (CLX)

The LX method encountered challenges related to segment length as larger segments might lack homogeneity. Addressing this issue, Leblanc et al. (2005a) combined the gap size distribution and finite-length methods. In the CLX method, the gap size distribution method is used to assess within-segment foliage heterogeneity. Subsequently, the total clumping index is computed over n segments as

$$\Omega_{CLX}(\theta) = \frac{n \ln[\overline{P(\theta)}]}{\sum_{k=1}^{n} \ln[P_k(\theta)]/\Omega_{CCk}(\theta)} \tag{13}$$

where $\Omega_{CCk}(\theta)$ represents the element clumping index of segment k based on Chen and Cihlar (1995) and $P_k(\theta)$ is the gap fraction of segment k.

Clumping index from gap size distribution after Macfarlane et al. (2007)

This method is based on utilizing distinct fractions of foliage cover (f_f, representing the ground area proportion covered by the vertical projection of foliage and branches, as defined by Walker and Tunstall (1981)) and crown cover (f_c) (Macfarlane et al., 2007). The calculation for the clumping index is as follows:

$$\Omega_M(0) = \frac{(1-\phi)\ln(1-f_f)}{\ln(\phi) f_f} \tag{14}$$

Crown porosity (ϕ, the inverse of canopy cover) is determined by Eq. (15):

$$\phi = 1 - \frac{f_f}{f_c} \tag{15}$$

Clumping index from the empirical equations by Kucharik et al. (1999)

Kucharik et al. (1999) formulated an empirical equation to estimate the clumping index for varying view angles, represented as:

$$\Omega_K(\theta) = \frac{\Omega_{K,max}}{1+b \exp[-k(\theta)^p]} \tag{16}$$

and

$$p = -0.461\chi + 3.8 \tag{17}$$

where χ denotes the ratio of crown depth to crown diameter, k is set to 2.2, and the value of b is determined by rearranging Eq. (17) and using a known $\Omega_K(\theta)$ value (e.g. θ=0°).

Apparent clumping

The approach introduced by Ryu et al. (2010b) involves two slightly different ways for calculating the effective LAI across multiple samples. The ratio between these methods can be employed as an "apparent" clumping index:

$$\Omega_{app} = \frac{2\int_0^{\pi/2} -[\ln \overline{P(\theta)}]cos\theta sin\theta d\theta}{2\int_0^{\pi/2} -[\overline{\ln P(\theta)}]cos\theta sin\theta d\theta}. \quad (18)$$

2.3.2 Measurements and data processing

Measurements for study **II** were conducted at two locations in Järvselja, involving a deciduous RAMI birch stand and an evergreen RAMI pine stand, over contrasting periods in the growing season, specifically during the peak season and again in the off-season.

DHPs were taken at nine sampling points within each stand under diffuse illumination conditions. The raw hemispherical images underwent processing using the freeware program HSP following Lang et al. (2010). This involved obtaining above-canopy blue channel references from each below-canopy image. The LinearRatio method by Cescatti (2007) was implemented, dividing below-canopy radiance images by above-canopy reference images to calculate gap fraction images. The resulting gap fraction data were converted to 8-bit bitmap images for use in TRACWin. Gamma was set to 1.0, with thresholds at values 0 and 254 on an 8-bit digital scale; pixels between these thresholds were treated as mixed by TRACWin. Clumping index estimates (Ω_{CC}, Ω_{LX} and Ω_{CLX}) were calculated using a segment length of 15°. Zenith angles within the range of 10°–80°, corresponding to LAI-2000 rings, were selected for subsequent processing and reporting.

DCPs were captured at the same sampling plots as DHPs, under clear sunlit conditions. To estimate the proportions of within- and between-crown gaps from the images, a method based on mathematical morphology, as outlined by Korhonen and Heikkinen (2009), was employed. The clumping index at θ=0° was determined following the approach of Macfarlane et al. (2007), and the values across all view zenith angles were calculated as Ω_K.

LAI-2000 measurements were obtained at the same locations as DHPs and DCPs, utilizing diffuse light conditions. Apparent clumping was computed using the approach proposed by Ryu et al. (2010b).

TRAC instrument measurements were successful only in the peak season; off-season measurements were hindered by the low position of the sun and insufficient direct light intensity, which prevented the reliable estimation of gap

fractions. The TRAC instrument was used under cloudless conditions along five 60–90 m long segments in each stand. To cover a broad range of view angles (θ), TRAC measurements were conducted at 30-minute intervals throughout half a day along each transect. For reference measurements, TRAC sensors were positioned at the center of nearby sunflecks at the beginning of each measurement series. Measurements in both stands were taken at an approximate height of 0.5 m above the forest floor. Measurements from individual transects were combined and then processed using TRACWin software (Leblanc, 2008). Clumping index values were estimated using the Ω_{CC}, Ω_{LX} and Ω_{CLX} methods.

2.4 Applicability under increased CO_2

The EucFACE facility comprises six 25 m circular plots (referred to as 'rings'), each featuring a walk-up tower at its center that extends to canopy's top. Among these rings, three are exposed to the normal ambient CO_2 concentration (~405 µmol mol^{-1}), while the remaining three experience an elevated concentration (ambient CO_2 + 150 µmol mol^{-1} during daylight hours).

For study **III**, LIA measurements using the digital camera method were performed in each ring, covering the entire vertical span of the tree crowns. The inclination angle of more than 400 leaves were measured in each ring and fitted to a beta distribution, as described in section 2.2.1. Vertical profiles of the clumping index were obtained from DHPs captured from the walk-up towers at the center of each ring. Reference DHPs were taken at the top of each tower, above the tree canopy. Gap fraction profiles were extracted using the DHP software (v4.5; Canada Centre for Remote Sensing, Ottawa, ON, Canada) by using a blue channel at a view zenith angle of 57°. The clumping index was calculated using the Ω_{CLX} method detailed in section 2.3.1.

The difference in leaf inclination angle distributions between ambient and elevated rings was assessed thorough Kolmogorov-Smirnov and Anderson-Darling tests (Massey, 1951; Anderson and Darling, 1952). The tests were applied on original measurements obtained from the digital images captured in the field. The significance level was established at 0.005 and results falling within the range of $0.005 < p < 0.05$ were considered marginally significant.

To evaluate the impact of measurement uncertainty in leaf inclination angles, 10 000 artificial leaf inclination angle datasets were generated for each of the rings as well as merged ambient and elevated CO_2 subsets. These datasets were of the same size as their respective original datasets, and they were created by randomly selecting values from the beta distribution fitted to original dataset. Additionally, each measurement was randomly adjusted by an increase or decrease of 0–5°, and the corresponding fitted beta distributions and G-functions were obtained.

3. RESULTS AND DISCUSSION

3.1 Leaf inclination angle distribution

3.1.1 Robustness of the leveled digital photography method

Study **I** showed the leveled digital photography method to be quite robust in terms of user experience and subjectivity, generally yielding comparable leaf inclination angle distributions across users (table 2). Of the four measured image sets, all ten users estimated planophile leaf inclination distribution for Moreton Bay chestnut (*Castanospermum australe*). Measurements of grey alder (*Alnus incana*) resulted in planophile distributions from most users, with two differing plagiophile results. Trailing lantana (*Lantana montevidensis*) was measured to have a uniform leaf inclination angle distribution by nine users, with one user achieving a spherical result. For this species, achieving the recommended sample size proved to be challenging due to a smaller number of suitable leaves on the photos, which can affect the results.

The only image set for which different users obtained strongly varying leaf inclination angle distributions was of European olive (*Olea europaea*). It is a species with a distinct long and narrow shape of leaves. When searching for leaves oriented perpendicular to the viewing direction, leaves with such shape are easier to be misidentified. The two experienced users obtained similar results from their measurements for *Olea europaea*, so in this case the discrepancy between the remaining results is most likely due to a lack of familiarity with the method. Despite this inconsistency, the leveled digital photography method remains generally robust for most broadleaf species, with caution advised for plants with elongated leaves.

*Table 2. Leaf inclination angle distribution types obtained through the multi-user comparison of the leveled digital camera method for four broadleaf tree species. PL – planophile, PG – plagiophile, U – uniform, S – spherical. Experienced users are marked in bold. Adopted from Article **I**.*

	User 1	User 2	User 3	**User 4**	User 5	**User 6**	User 7	User 8	User 9	User 10
Alnus incana	PL	PL	PL	PL	PG	PL	PG	PL	PL	PL
Castanospermum australe	PL	PL	PL	PL	PL	PL	PL	PL	PL	PL
Lantana montevidensis	U	U	U	U	U	U	S	U	U	U
Olea europaea	S	PG	PG	S	U	S	U	PG	U	U

3.1.2 Changes with season, height in the canopy, and light exposure

Throughout the growing season, the leaf inclination angle distributions of different tree species revealed distinct patterns. Norway maple (*Acer platanoides*) exhibited a strong planophile distribution throughout most of the growing season, with notable differences at the canopy top during spring and autumn (Fig. 4). The leaves emerged oriented downward and became more horizontally oriented when fully expanded. This change was visible only at the canopy top due to earlier leaf expansion in the lower canopy sections, completed by the first data collection event. The canopy remained planophile until late summer, when senescence begins at the canopy top, leading to a shift back to plagiophile.

Horse chestnut (*Aesculus hippocastanum*) consistently maintained a predominantly plagiophile orientation with minimal height variation (Fig. 5). However, a noticeable shift toward planophile occurred in June, particularly evident at the canopy top. This change is attributed to the upward expansion of initially downward-pointing leaves during spring, gradually becoming more horizontally oriented by early summer. The early senescence and short leaf longevity of *Aesculus hippocastanum* likely contribute to the turn toward plagiophile, especially in the exposed canopy top (Augspurger and Bartlett, 2003).

Grey alder (*Alnus incana*) underwent minor but continuous changes throughout the growing season. The leaf inclination angle distribution was strongly planophile in spring, remaining so for most of the season, but with a continuous decrease in the proportion of horizontally oriented leaves. Some change toward uniform or plagiophile was observed in autumn, possibly influenced by increasing lamina size resulting in heavier load on petiole and steeper leaf inclination angles (Niklas, 1991). The greatest change occurred at the canopy top, where the proportion of horizontally oriented leaves in spring noticeably exceeded that at lower canopy levels.

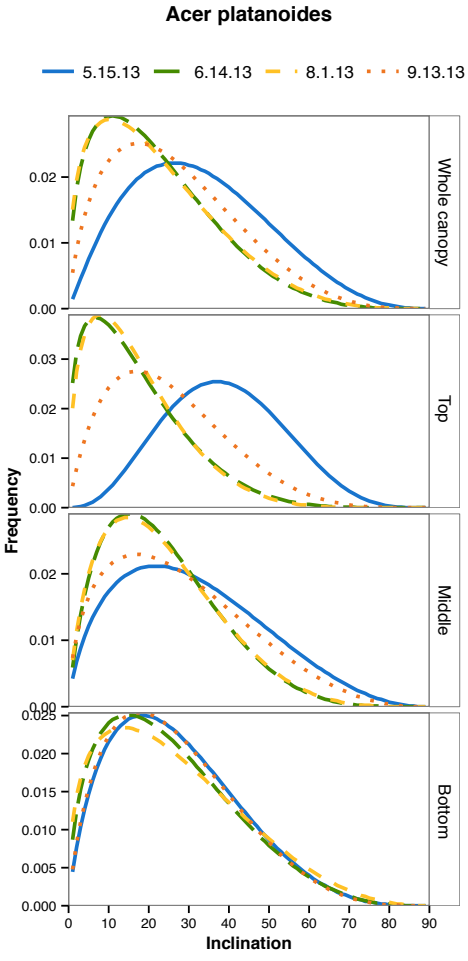

Figure 4. Seasonal and vertical variation of leaf inclination angle distribution for Acer platanoides*. Adopted from Article* ***I****.*

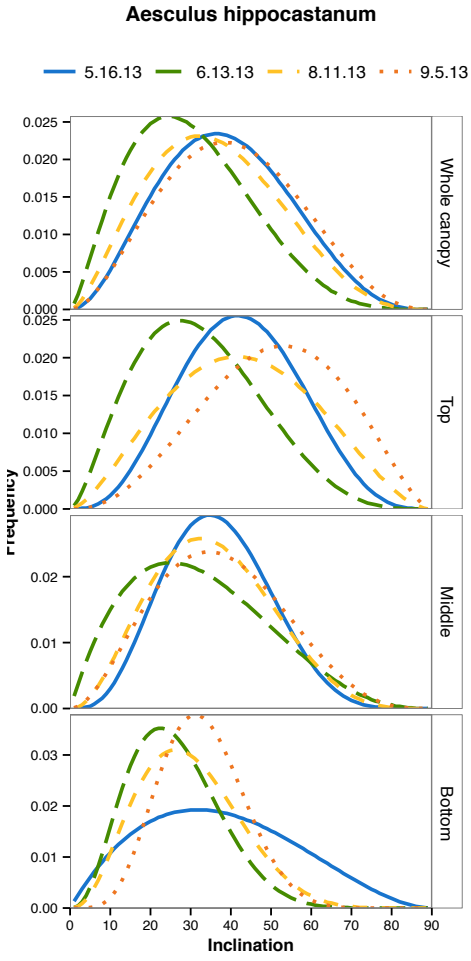

Figure 5. Seasonal and vertical variation of leaf inclination angle distribution for Aesculus hippocastanum*. Adopted from Article* ***I****.*

Eurasian aspen (*Populus tremula*) displayed a planophile orientation in spring and mostly uniform distribution throughout the rest of the growing season. The leaves initially appeared somewhat horizontally oriented, with the bottom of the canopy retaining some horizontal orientation due to limited light availability (Niinemets, 1998). By the end of the season, the top turned plagiophile, likely due to leaf aging.

Silver birch (*Betula pendula*) (Fig. 6) remained erectophile throughout the growing season, with minimal seasonal or vertical variation. The only noticeable change occurred at the bottom of the canopy during peak growing season when downward hanging leaves lifted slightly, changing the distribution to plagiophile, possibly due to reduced light availability.

The observed leaf inclination angle distributions align with the previous notions where shade-intolerant species have steeper leaf inclination angles, while shade-tolerant species exhibit more horizontally oriented leaves (McMillen and McClendon, 1979; Pearcy et al., 2004). Changes in leaf inclination angle distribution are most significant in early spring, with the direction of change either upwards or downwards depending on the cause. Leaf unfolding tends to decrease inclination angles, while petiole lengthening and increased lamina mass result in steeper angles. The theoretical approximation for leaf inclination angles remains consistent for most species during the later part of the growing season, with a potential exception during late summer when angles may become steeper, possibly due to the increases in lamina mass and area along with leaf age (Gordon and Promnitz, 1976; Hamerlynck and Knapp, 1996). Seasonal changes are more pronounced at the canopy top and bottom than in the middle of the canopy, with no other notable patterns found for the differences in leaf inclination angle distributions at different heights within the canopy for the studied tree species.

With the five tree species studied in open well-lit locations, the influence of different light exposure on the leaf inclination angle distribution was also investigated by including additional four species growing in natural forests. For *Betula pendula*, the only species measured both in the open and in a forest, it was observed that at the canopy top, the distribution remained erectophile regardless of the growing conditions. However, with decreasing height, there was a gradual shift towards more horizontally oriented leaf angles in the forest, resulting in a planophile distribution at the bottom (Fig. 7). This pattern aligns with previous findings and suggests that varying light exposure at different heights within the canopy contributes to these changes (e.g. Hutchinson et al., 1986; Hollinger, 1989; Niinemets, 1998). Excessive light at the canopy top can lead to water stress and photo-inhibition of photosynthesis, prompting the need for steeply inclined leaves to mitigate exposure and enhance light penetration into the canopy (Ball et al., 1988; King, 1997). In contrast, horizontally oriented leaves at the canopy bottom efficiently intercept light at lower intensities (Ford and Newbould, 1971). In environments with higher light availability, such stratification becomes unnecessary, resulting in reduced variation in leaf inclination angles, as seen in the park-grown *Betula pendula*.

Red maple (*Acer rubrum*) and northern red oak (*Quercus rubra*) exhibited smaller vertical variations in leaf inclination angles compared to *Betula pendula*. Both species displayed predominantly planophile leaf inclination angle distributions throughout the season, with a plagiophile distribution in the spring before full leaf expansion, but minimal seasonal variation later. Despite slightly less horizontal leaf inclination angles in the upper canopy, a planophile distribution meant there was no strong exposure-related vertical difference. Yellow birch (*Betula alleghaniensis*), identified as a suppressed tree species in Harvard Forest, also displayed a planophile leaf inclination angle distribution across all heights, probably due to limited light availability. The lack of seasonal change, except at the bottom of the canopy, could be attributed to earlier budburst and leaf growth for sub-canopy tree species (Augspurger, 2008).

While supporting a uniformly planophile canopy may not be the most effective strategy for maximizing single tree productivity, it provides a competitive advantage over other tree species with steeper leaves. The findings for *Betula pendula* confirm the vertical variation of leaf inclination angles reported in previous studies (e.g. Kull et al., 1999; Utsugi et al., 2006), also emphasizing the significant impact of light exposure on leaf orientation. Thus, it is recommended to obtain actual leaf inclination angle measurements whenever possible to comprehensively understand the ecological dynamics of tree species in various environments.

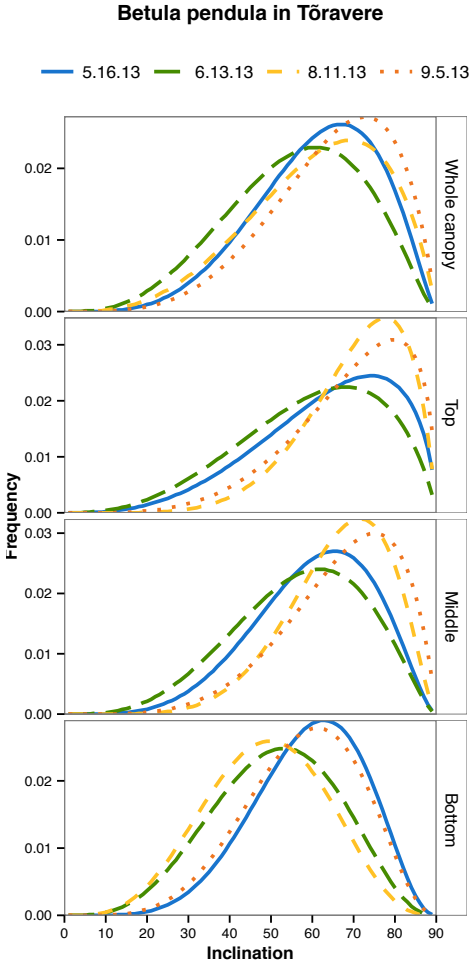

Figure 6. Seasonal and vertical variation of leaf inclination angle distribution for Betula pendula *in Tõravere. Adopted from Article* ***I****.*

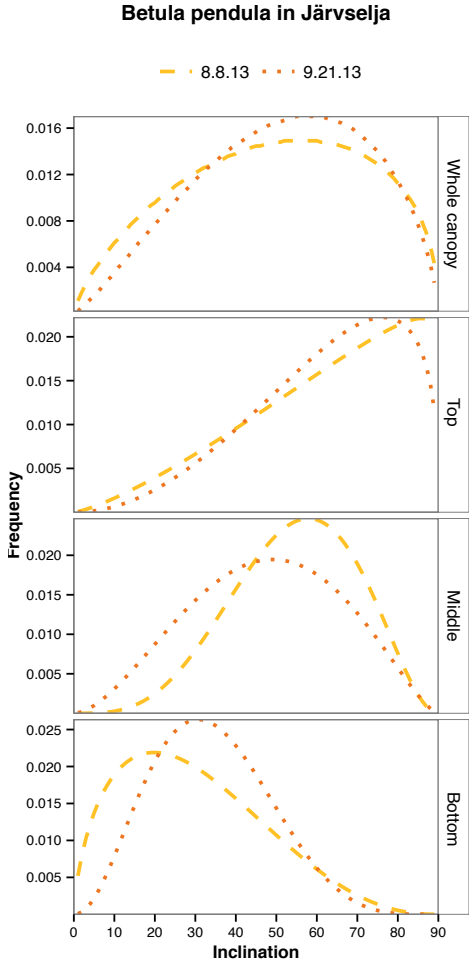

Figure 7. Seasonal and vertical variation of leaf inclination angle distribution for Betula pendula *in Järvselja. Adopted from Article* ***I****.*

3.1.3 Changes under elevated CO_2

In all rings investigated in study **III**, there was an erectophile, highly skewed leaf inclination angle distribution. While no significant differences were found in leaf inclination angle distributions among individual rings within each treatment group (ambient CO_2 and elevated CO_2), marginal significance was observed between rings under different CO_2 concentrations, with elevated CO_2 rings showing a higher proportion of steeper leaf angles (Fig. 8). Additionally, a significant difference was detected between the aggregated leaf angle measurements from rings with ambient and with elevated CO_2 concentrations. Accounting for measurement uncertainty revealed an overlap of G-function values between artificial leaf inclination angle datasets per each CO_2 treatment.

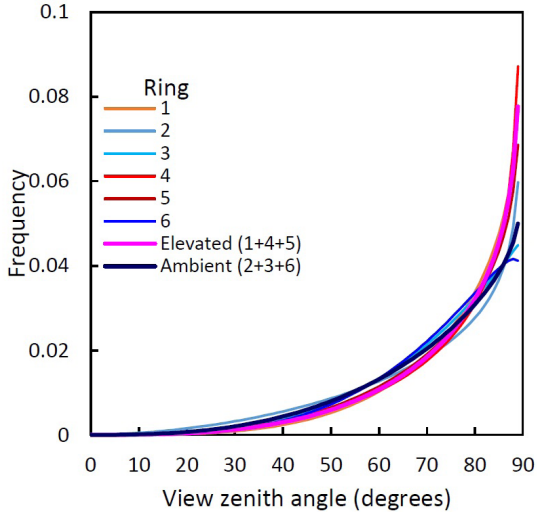

*Figure 8. Fitted beta distributions of leaf angle inclinations for each of the free-air CO_2 enrichment rings, along with the aggregated ambient and elevated CO_2 datasets. Adopted from Article **III**.*

The causes for the steeper leaf inclination angles exhibited in rings with elevated CO_2 might include increased leaf mass by area (Feng et al., 2015; Wujeska-Klause et al., 2019) and longer leaf lifespans (Duursma et al., 2016) in such conditions. However, when considering measurement uncertainties, an overlap was found in resulting G-function values for different CO_2 treatments, indicating that the observed changes were within expected natural variability. The lack of significant modification in leaf inclination angle distribution with elevated CO_2 implies that leaf orientation data collected under current CO_2 concentrations, such as presented in studies **IV** and **V**, remain useful for modeling surface fluxes under changing CO_2 conditions.

3.2 Foliage clumping

3.2.1 Foliage clumping method evaluation

Multi-angle gap fraction values in study **II** were measured using LAI-2000 and TRAC instruments and DHP; a single value was obtained with DCP (Fig. 9). In the RAMI pine stand, a slight difference in values between peak and off-season was noted (Fig. 9a), attributed to natural needle loss in autumn (Lang et al., 2017). LAI-2000 and DHP showed strong agreement during off-season measurements as well as peak season, where TRAC data followed a similar trend, albeit with a small offset. DCP displayed a stable fit with LAI-2000 during both measurement times.

In the RAMI birch stand, peak and off-season P(θ) values exhibited a significant difference (Fig. 9b). During peak season, TRAC and DHP had the strongest agreement, while LAI-2000 and DCP yielded higher values. Off-season measurements indicated a greater P(θ) from DCP, likely due to issues in classifying mixed pixels. Overall, LAI-2000 consistently provided the highest gap fraction values in all cases, except for the off-season DCP in the birch stand. TRAC consistently provided the smallest values, attributed to its tendency to underestimate small gap contributions due to sensor resolution (Leblanc et al., 2005a; Kucharik et al., 1997). This trend aligns with previous observations in the literature (Ryu et al., 2010a).

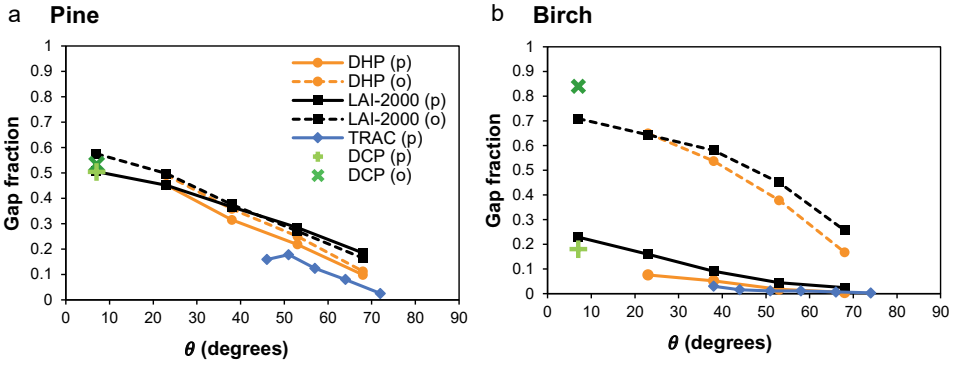

Figure 9. Total gap fraction comparison between TRAC, DHP, DCP and LAI-2000 sensors in the pine (a) and birch (b) stand. P marks peak season and o denotes off-season. Adopted from Article ***II****.*

Figures 10 and 11 depict the variation in clumping index across different methods and zenith angles for the pine and birch stands, respectively. Only apparent clumping is presented as a single value across all zenith angles. As a general trend, Ω increases with view zenith angle, as concluded for various land cover types in previous studies (Kucharik et al., 1997; Fang et al., 2014).

Results from different methods exhibit significant variability, with CLX and LX methods consistently resulting in smaller Ω values, indicative of more clumped foliage, while apparent clumping, CC, Macfarlane and Kucharik methods tend to

provide greater Ω values at given zenith angles, closer to a random foliage distribution. The CC method, which is known to generally underestimate LAI (Leblanc et al., 2005a), has been repeatedly observed to provide significantly greater clumping index values compared to LX and CLX methods both with field data (Pisek et al., 2011b) as well as simulated photographs (Gonsamo and Pellikka, 2009; Leblanc and Fournier, 2014).

With DHP estimates, there are considerable differences between calculation methods, with the CC method consistently providing higher clumping index values, while LX and CLX methods are more comparable to each-other. TRAC estimates follow a similar pattern, with a smaller variation in values. Notably, the results from both DHP and TRAC are very close using the CC method, while with LX and CLX they differ more. There is also a correspondence of CC clumping index estimates with apparent clumping and Kucharik method, which echoes findings from Ryu et al. (2010b).

The clumping index estimates obtained with TRAC instrument are less consistent compared to other approaches. Although Ω generally increases with zenith angle, a decrease is observed in the pine stand (Fig. 10a). This can be attributed to the instrument's low resolution that combines the numerous small gaps present in a conifer canopy into larger gaps. This issue seems specific to the combination of the TRAC instrument and the LX method, which requires a random distribution of foliage within a segment.

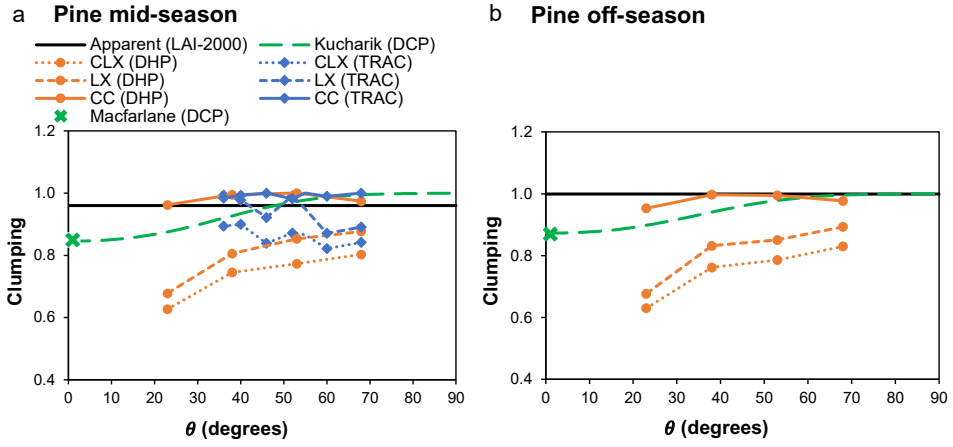

Figure 10. Element clumping index Ω with view zenith angle θ at the pine stand measured from TRAC, DHP, DCP and LAI-2000 at the middle of the growing season (a) and off-season (b). Adopted from Article ***II****.*

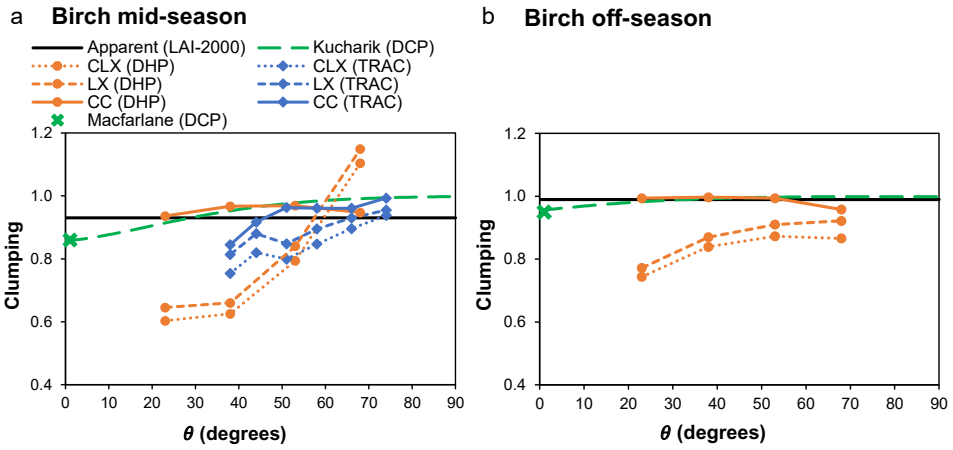

Figure 11. Element clumping index Ω with view zenith angle θ at the birch stand measured from TRAC, DHP, DCP and LAI-2000 at the middle of the growing season (a) and off-season (b). Adopted from Article ***II****.*

In the pine stand, the difference between mid- and off-season measurements remains consistently small, as shown in Figure 10. Estimates from the Macfarlane and Kucharik methods exhibit notable agreement between seasons. Other methods can show variations up to 10%, with off-season clumping index values consistently surpassing those in mid-season. In the birch stand (Fig. 11), clumping index values are markedly higher during the off-season, aligning with the established notion that Ω decreases with canopy development and increases during the senescent phase of the season (Fang et al., 2014; Pisek et al., 2013b). An exception is observed for the logarithmic estimations from DHP at the highest view angle (θ=68°), where mid-season estimates considerably exceed off-season values, likely due to a very small gap fraction value (0.005), impacting the reliability of Ω calculations. Notably, the CC method displays the most consistency and is less affected by the lower resolution of TRAC, which likely cannot measure the small gap fraction accurately. During the leaves-off season (Fig. 11b), differences between clumping index values obtained by various methods tend to be smaller overall.

In previous studies, CLX has often been regarded as the most accurate method for calculating Ω (Pisek et al., 2011b; Leblanc and Fournier, 2014), while methods like apparent clumping, Kucharik, and CC consistently provide high clumping index values across different forest types and measurement times. Consequently, CC, Kucharik, and apparent clumping methods serve as an upper boundary for Ω, representing the minimum clumping to consider during LAI calculations. On the other hand, CLX estimates may be closer to the real value, especially during the leaves-on period. It is noteworthy that estimates from different methods converge around θ of 50°–60°, where uncertainty related to the often unknown G-function is minimized. CLX estimates for θ ~57° might be

particularly suitable for validating foliage clumping maps from airborne/satellite platforms (Pisek and Oliphant, 2013; Pisek et al., 2013b, 2015).

It is encouraging to observe that digital photography, particularly DHP, provides reliable clumping index estimates. As digital photography is generally readily available and does not require specialized instruments, this allows for easier clumping data collection.

3.2.2 Foliage clumping under elevated CO2

In the EucFACE experiment in Australia (study **III**), vertical profiles of gap fraction demonstrated an increase in gap with distance from the ground across all rings, indicative of differences in tree density and heights of individual trees. No noticeable distinction was observed in the vertical profiles of gap fraction between rings exposed to ambient and elevated CO_2 levels. Similarly, foliage clumping followed the vertical profiles of gap fraction, with the smallest clumping index values and the greatest range observed at the top of the canopy and a smaller range in clumping index values in the random distribution case near the ground (Fig. 12). Like the gap fraction, the vertical profiles of foliage clumping index did not show any clear difference between rings exposed to ambient CO_2 levels and those exposed to elevated CO_2 concentrations.

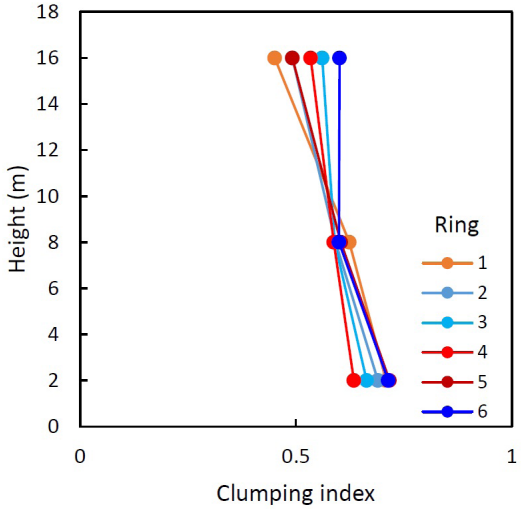

*Figure 12. Vertical profiles of foliage clumping index for each of the free-air CO_2 enrichment (FACE) rings. Adopted from Article **III**.*

The vertical profiles and variability in foliage clumping across different rings resembled measurements from other *Eucalyptus*-dominated sites in Australia (Pisek et al., 2015; Woodgate et al., 2017). Consistent clumping index estimates were most notable at 8 meters above ground level, corresponding to the lower limit of tree canopies. Variability in clumping index was higher near the ground due to occasional shrub presence, while the greatest variation occurred at 16

meters height, where large gaps in the upper canopy were fully exposed. The findings underscore the importance of obtaining enough plots and considering non-linear clumping effects when scaling to the landscape level (Ryu et al., 2010b). Additionally, the lack of a clear response in foliage clumping to elevated CO_2 suggests that existing maps derived from Earth Observation data (e.g. Chen et al., 2005; Pisek et al., 2015; Jiao et al., 2018) may suffice for carbon and water cycle modeling under climate change.

4. CONCLUSIONS

Based on the work presented in this thesis, the following conclusions can be made.

- The leveled digital photography method is a robust means to measure leaf inclination angles. Even though extra attention should be paid while measuring long and narrow leaves, in most cases experience is not required to obtain reliable results with this method that also benefits from being relatively simple and affordable.
- Clumping index calculation methods based on logarithmic average and its combination with gap size distribution, particularly when used with data from digital hemispherical photos, provide the most pronounced clumping results. These should be considered more accurate than approaches such as calculation based on gap size distribution or apparent clumping, which rather provide higher values, suitable for treating as the minimum clumping to be taken into account.
- The leaf inclination angle distribution is highly variable and dependent on season, height in the canopy, and light exposure. Seasonally, leaf inclination angle distribution varies the most in spring and for some species, late summer, remaining relatively constant over the rest of the growing season. The variation is most visible at the top of canopy, whereas middle and bottom parts of the canopy change less throughout the season. The effect of different light exposure on leaf inclination angle distribution is particularly strong on species with steeper leaf inclination angles, while canopies with more horizontally oriented leaves vary less.
- Seasonal variability should also be considered in clumping index measurements, where even evergreen needleleaf canopies display smaller clumping index values (i.e. the canopy is more clumped) during the growing season. The same trend with a much larger difference in values is present in deciduous canopies.
- Elevated CO_2 concentration does not have a significant effect on neither leaf inclination angle distribution nor clumping index, indicating that current data available on each parameter may remain relevant with the increasing atmospheric CO_2 in the future.

To summarize, this study first assessed the means of measuring the leaf inclination angles and clumping index by verifying the robustness of a simple and accessible method of LIA measurement (**I**) as well as providing the most comprehensive comparison of clumping index calculation methods and measurement instruments up to date (**II**). The importance of obtaining actual information on each parameter and particularly LIAD was then shown by describing their variability with season, height in the canopy and light exposure (**I**, **II**). The most expansive dataset of leaf inclination angles currently available was provided, to

be used by the wider community (**IV**, **V**). Finally, it was shown that the collected datasets will likely stay relevant under the changing climate conditions even with increasing atmospheric CO_2 (**III**). Given the significant impact of leaf inclination angles and the clumping index on biomass productivity and radiative transfer, the findings of this thesis hold substantial potential to advance future modeling efforts.

REFERENCES

Anderson, T.W., Darling, D.A., 1952. Asymptotic theory of certain "goodness of fit" criteria based on stochastic processes. *Annals of Mathematical Statistics*, 23, 193–212.

Anten, N.P.R., 2005. Optimal photosynthetic characteristics of individual plants in vegetation stands and implications for species coexistence. *Annals of Botany*, 95, 495–506.

Augspurger, C.K., 2008. Early spring leaf out enhances growth and survival of saplings in a temperate deciduous forest. *Oecologia*, 156, 281–286.

Augspurger, C.K., Bartlett, E.A., 2003. Differences in leaf phenology between juvenile and adult trees in a temperate deciduous forest. *Tree Physiology*, 23, 517–525.

Bailey, B.N., Mahaffee, W.F., 2017. Rapid measurement of the tree-dimensional distribution of leaf orientation and the leaf angle probability density function using terrestrial LiDAR scanning. *Remote Sensing of Environment*, 194, 63–76.

Baldocchi, D.D., Wilson, K.B., Gu, L., 2002. How the environment, canopy structure and canopy physiological functioning influence carbon, water and energy fluxes of a temperate broadleaved deciduous dorest – an assessment with the biophysical model CANOAK. *Tree Physiology*, 22, 1065–1077.

Ball, M.C., Cowan, I.R., Farquhar, G.D., 1998. Maintenance of Leaf Temperature and the Optimisation of Carbon Gain in Relation to Water Loss in a Tropical Mangrove Forest. *Australian Journal of Plant Physiology*, 15, 263–276.

Baret, F., de Solan, B., Lopez-Lozano, R., Ma, K., Weiss, M., 2010. GAI estimates of row crops from downward looking digital photos taken perpendicular to rows at 57.5° zenith angle: Theoretical considerations based on 3D architecture models and application to wheat crops. *Agricultural and Forest Meteorology*, 150 (11), 1393–1401.

Bonan, G.B., Patton, E.G., Finnigan, J.J., Baldocchi, D.D., Harman, I.N., 2021. Moving beyond the incorrect but useful paradigm: reevaluating big-leaf and multilayer plant canopies to model biosphere-atmosphere fluxes – a review. *Agricultural and Forest Meteorology*, 306, 108435.

Braghiere, R.K., Quaife, T., Black, E., Ryu, Y., Chen, Q., De Kauwe, M.G., Baldocchi, D., 2020. Influence of sun zenith angle on canopy clumping and the resulting impacts on photosynthesis. *Agricultural and Forest Meteorology*, 291, 108065.

Canham, C.D., Denslow, J.S., Platt, W.J., Runkle, J.R., Spies, T.A., White, P.S., 1990. Light regimes beneath closed canopies and tree-fall gaps in temperate and tropical forests. *Canadian Journal of Forest Research*, 20, 620–631.

Cescatti, A., 2007. Indirect estimates of canopy gap fraction based on the linear conversion of hemispherical photographs: methodology and comparison with standard thresholding techniques. *Agricultural and Forest Meteorology*, 143, 1–12.

Chen, J.M., Cihlar, J., 1995. Plant canopy gap-size analysis theory for improving optical measurements of leaf-area index. *Applied Optics*, 34, 6211–6222.

Chen, J.M., 1996. Optically based methods for measuring seasonal variation of leaf area index in boreal conifer stands. *Agricultural and Forest Meteorology*, 80 (2–4), 135–163.

Chen, J.M., Menges, C.H., Leblanc, S.G., 2005. Global mapping of foliage clumping index using multi-angular satellite data. *Remote Sensing of Environment*, 97, 447–457.

Chen, J.M., Mo, G., Pisek, J., Liu, J., Deng, F., Ishizawa, M., Chan, D., 2012. Effects of foliage clumping on the estimation of global terrestrial gross primary productivity. *Global Biogeochemical Cycles*, 26 (1), GB1019.

Chianucci, F., Disperati, L., Guzzi, D., Bianchini, D., Nardino, V., Lastri, C., Rindinella, A., Corona, P., 2016. Estimation of canopy attributes in beech forests using true colour digital images from a small fixed-wing UAV. *International Journal of Applied Earth Observation and Geoinformation*, 47, 60–68.

Davi, H., Bouriaud, O., Dufrene, E., Soudani, S., Pointaillier, J.Y., le Maire, G., Francois, C., Breda, N., Granier, A., le Dantec, V., 2006. Effect of aggregating spatial parameters on modelling forest carbon and water fluxes. *Agricultural and Forest Meteorology*, 139, 269–287.

De Wit, C.T., 1965. Photosynthesis of Leaf Canopies. Agricultural Research Report No 663, Wageningen.

Disney, M., Burt, A., Calders, K., Schaaf, C., Stovall, A., 2019. Innovations in ground and airborne technologies as reference and for training and validation: terrestrial laser scanning (TLS). *Surveys in Geophysics*, 30, 937–958.

Duursma, R.A., Mäkelä, A., 2007. Summary models for light interception and light-use efficiency of non-homogeneous canopies. *Tree Physiology*, 27, 859–870.

Duursma, R.A., Gimeno, T.R., Boer, M.M., Crous, K.Y., Tjoelker, M.G., Ellsworth, D.S., 2016. Canopy leaf area of a mature evergreen Eucalyptus woodland does not respond to elevated atmospheric [CO_2] but tracks water availability. *Global Change Biology*, 22, 1666–1676.

Falster, D.S., Westoby, M., 2003. Leaf size and angle vary widely across species: what consequences for light interception? *New Phytologist*, 158, 509–525.

Fang, H., Li, W., Wei, S., Jiang, C., 2014. Seasonal variation of leaf area index (LAI) over paddy rice fields in NE China: intercomparison of destructive sampling, LAI-2200, digital hemispherical photography (DHP), and AccuPAR methods. *Agricultural and Forest Meterology*, 199–199, 126–141.

Fang, H., 2021. Canopy clumping index (Cl): A review of methods, characteristics, and applications. *Agricultural and Forest Meteorology*, 303, 108374.

Farrior, C.E., Tilman, D., Dybzinski, R., Reich, P.B., Levin, S.A., Pacala, S.W., 2013. Resource limitation in a competitive context determines complex plant responses to experimental resource additions. *Ecology*, 94, 2505–2517.

Feng, Z., Rütting, T., Pleijel, H., Wallin, G., Reich, P.B., Kammann, C.I., Newton, P.C.D., Kobayashi, K., Luo, Y., Uddling, J., 2015. Constraints to nitrogen acquisition of terrestrial plants under elevated CO_2. *Global Change Biology*, 21, 3152–3168.

Ford, E.D., Newbould, P.J., 1971. The Leaf Canopy of a Coppiced Deciduous Woodland: I. Development and Structure. *Journal of Ecology*, 59, 843–862.

Gastellu-Etchegorry, J.-P., Lauret, N., Yin, T., Landier, L., Kallel, A., Malenovsky, Z., Al Bitar, A., Aval, J., Benhmida, S., Qi, J., Medjdoub, G., Guilleux, J., Chavanon, E., Cook, B., Morton, D.C., Chrysoulakis, N., Mitraka, Z., 2017. DART: recent advances in remote sensing data modeling with atmosphere, polarization, and cholrophyll fluorescence. *IEEE Journal of Selected Topics in Applied Earth Observations and Remote Sensing*, 10, 2640–2649.

GCOS, 2016. The Global Observing System for Climate: Implementation Needs (GCOS-200). World Meteorological Organization. https://gcos.wmo.int/en/publications/gcos-implementation-plan2016 (accessed 23.07.2024)

Goel, N.S., Strebel, D.E., 1984. Simple beta distribution representation of leaf orientation in vegetation canopies. *Agronomy Journal*, 76, 800–802.

Gonsamo, A., Pellikka, P., 2009. The computation of foliage clumping index using hemispherical photography. *Agricultural and Forest Meteorology*, 149, 1781–1787.

Gordon, J.C., Promnitz, L.C., 1976. Photosynthetic and enzymatic criteria for the early selection of fast-growing Populus clones. In: Cannell, M.R.G., Last, F.T. (Eds.), *Tree Physiology and Yield Improvement, A Compendium of Papers Given at a Meeting Held Near Edinburgh in July* 1975. Academic Press, London, pp. 79–109.

Hamerlynck, E.P., Knapp, A.K., 1996. Early season cuticular conductance and gas exchange in two oaks near the western edge of their range. *Trees*, 10, 403–409.

He, L., Chen, J.M., Pisek, J., Schaaf, C.B., Strahler, A.H., 2012. Global clumping index map derived from the MODIS BRDF product. *Remote Sensing of Environment*, 119 (0), 118–130.

Hill, M.J., Roman, M.O., Shaaf, C.B., Hutley, L., Brannstrom, C., Etter, A., Hanan, N.P., 2011. Characterizing vegetation cover in global savannas with an annual foliage clumping index derived from the MODIS BRDF product. *Remote Sensing of Environment*, 115, 2008–2024.

Hollinger, D.Y., 1989. Canopy organization and foliage photosynthetic capacity in broad-leaved evergreen montane forest. *Functional Ecology*, 3, 13–24.

Hosoi, F., Omasa, K., 2009. Detecting seasonal change of broad-leaved woody canopy leaf area density profile using 3D portable LIDAR imaging. *Functional Plant Biology*, 36, 13–24.

Hutchinson, B.A., Matt, D.R., McMillen, R.T., Gross, L.J., Tajchman, S.J, Norman, J.M., 1986. The architecture of a deciduous forest canopy in eastern Tennessee, USA. *Journal of Ecology*, 74, 635–646.

Jiao, Z., Dong, Y., Schaaf, C.B., Chen, J.M., Roman, M., Wang, Z., Zhang, J., Ding, A., Erb, A., Hill, M.J., Zhang, X., Strahler, A., 2018. An algorithm for the retrieval of the clumping index (Cl) from the MODIS BRDF product using an adjusted version of the kernel-driven BRDF model. *Remote Sensing of Environment*, 209, 594–611.

Jonckheere, I., Fleck, S., Nackaerts, K., Muys, B., Coppin, P., Weiss, M., Baret, F., 2004. Methods for leaf area index determination. Part I: Theories, techniques and instruments. *Agricultural and Forest Meteorology*, 121, 19–35.

King, D.A., 1997. The Functional Significance of Leaf Angle in Eucalyptus. *Australian Journal of Botany*, 45, 619–639.

Korhonen, L., Heikkinen, J., 2009. Automated analysis of in situ canopy images for the estimation of forest canopy cover. *Forest Science*, 55, 323–334.

Koven, C.D., Knox, R.G., Fisher, R.A., Chambers, J.Q., Christoffersen, B.O., Davies, S.J., et al. 2020. Benchmarking and parameter sensitivity of physiological and vegetation dynamics using the functionally assembled terrestrial ecosystem simulator (FATES) at Barro Colorado Island, Panama. *Biogeosciences*, 17, 3017–3044.

Kucharik, C.J., Norman, J.M., Murdoch, L.M., 1997. Characterizing canopy nonrandomness with a multiband vegetation imager (MVI). *Journal of Geophysical Research*, 102, 29455–29473.

Kucharik, C., Norman, J.M., Gower, S.T., 1998. Measurements of leaf orientation, light distribution and sunlit area in a boreal aspen forest. *Agricultural and Forest Meteorology*, 91, 127–148.

Kucharik, C.J., Norman, J.M., Gower, S.T., 1999. Characterization of radiation regimes in nonrandom forest canopies: theory, measurements and a simplified modeling approach. *Tree Physiology*, 19, 695–706.

Kull, O., Broadmeadow, M., Krujit, B., Meir, P., 1999. Light distribution and foliage structure in an oak canopy. *Trees*, 14, 55–64.

Laisk, A., 1965. An improved photoelectric planimeter and a device for determining the orientation of leaves. In: *Questions on the radiation regime of plant cover*. Institute of Physics and Astronomy, Tartu, pp. 102–112 (in Russian).

Lang, A.R.G., 1973. Leaf orientation of a cotton plant. *Agricultural Meteorology*, 11, 37–51.

Lang, A.R.G., Xiang, Y., 1986. Estimation of leaf area index from transmission of direct sunlight in discontinuous canopies. *Agricultural and Forest Meteorology*, 37, 229–243.

Lang, M., Kuusk, A., Mõttus, M., Rautiainen, M., Nilson, T., 2010. Canopy gap fraction estimation from digital hemispherical images using sky radiance models and a linear conversion method. *Agricultural and Forest Meteorology*, 150, 20–29.

Lang, M., Nilson, T., Kuusk, A., Pisek, J., Korhonen, L., Uri, V., 2017. Digital photography for tracking the phenology of an evergreen conifer stand. *Agricultural and Forest Meteorology*, 246, 15–21.

Lau, A., Calders, K., Bartholomeus, J., Martius, C., Raumonen, P., Herold, M., Vicari, M., Sukhdeo, H., Singh, J., Goodman, R.C., 2019. Tree biomass equations from terrestrial LiDAR point clouds of forests. *IEEE Transactions on Geoscience and Remote Sensing*, 58, 3057–3070.

Lawrence, D.M., Fisher, R.A., Koven, C.D., Oleson, K.W., Swenson, S.C., Bonan, G., Collier, N., Ghimire, B., van Kampenhout, L., Kennedy, D., Kluzek, E., et al., 2019. The community land model version 5: description of new features, benchmarking, and impact of forcing uncertainty. *Journal of Advance in Modeling Earth Systems*, 11, 4245–4287.

Leblanc, S.G., 2002. Correction to the plant canopy gap-size analysis theory used by the Tracing Ratiation and Architecure of Canopies instrument. *Applied Optics*, 41, 7667–7670.

Leblanc, S.G., Chen, J.M., Fernandes, R., Deering, D.W., Conley, A., 2005a. Methodology comparison for canopy structure parameters extraction from digital hemispherical photography in boreal forests. *Agricultural and Forest Meteorology*, 129, 187–207.

Leblanc, S.G., Chen, J., White, H.P., Latifovic, R., Lacaze, R., Roujean, J.-L., 2005b. Canada-wide foliage clumping index mapping from multiangular POLDER measurements. *Canadian Journal of Remote Sensing*, 31 (5), 364–376.

Leblanc, S.G., 2008. DHP-TRACWin manual, version 1.0.1 (30 January 2008). Natural Resources Canada. Canada Centre for Remote Sensing, Ottawa.

Leblanc, S.G., Fournier, R.A., 2014. Hemispherical photography simulations with an architectural model to assess retrieval of leaf area index. *Agricultural and Forest Meteorology*, 194, 64–76.

Lemeur, R., Blad, B.L., 1974. A critical review of light models for estimating the shortwave radiation regime of plant canopies. *Agricultural and Forest Meteorology*, 14, 255–286.

Lerdau, M., Holbrook, N.M., Mooney, H.A., Rich, P.M., Whitebeck, J.L., 1992. Seasonal patterns of acid fluctuations and resource storage in the arborescent cactus Opuntia exelsa in relation to light availability and size. *Oecologia*, 92, 166–171.

LI-COR, Inc., 2010. LAI-2200 Plant Canopy Analyzer, Instruction Manual. 10-23, LAI-COR, Inc., Lincoln, Nebraska 68504 USA.

Lunka, P., Patil, S.D., 2016. Impact of tree planting configuration and grazing restriction on canopy interception and soil hydrological properties: implications for flood mitigation in silvopastoral systems. *Hydrological Processes*, 30 (6), 945–958.

Macfarlane, C., Hoffman, M., Eamus, D., Kerp, N., Higginson, S., McMurtrie, R., Adams, M., 2007. Estimation of leaf area index in eucalypt forest using digital photography. *Agricultural and Forest Meteorology*, 8, 25–38.

Massey, F.J., 1951. The Kolmogorov-Smirnov Test for Goodness of Fit. *Journal of the American Statistical Association*, 46, 68–78.

McMillen, G.G., McGlendon, J.H., 1979. Leaf angle: an adaptive feature of sun and shade leaves. *Botanical Gazette*, 140, 437–442.

Monsi, M., Saeki, T., 1953. Über den Lichtfaktor in den Pflanzengesellschaften und seine Bedeutung für die Stoffproduktion. *Japanese Journal of Botany*, 14, 22–52.

Monsi, M., Saeki, T., 2005. On the factor light in plant communities and its importance for matter production. *Annals of Botany*, 95, 549–567.

Myneni, R.B., Ross, J., Asrar, G., 1989. A review on the theory of photon transport in leaf canopies. *Agricultural and Forest Meteorology*, 45 (1–2), 1–153.

Nasahara, K.N., Muraoka, H., Nagai, S., Mikami, H., 2008. Vertical integration of leaf area index in a Japanese deciduous broad-leaved forest. *Agricultural and Forest Meteorology*, 148 (6–7), 1136–1146.

Niinemets, Ü., 1998. Adjustment of foliage structure and function to a canopy light gradient in two co-existing deciduous trees. Variability in leaf inclination angles in relation to petiole morphology. *Trees*, 12, 446–451.

Niinemets, Ü., 2010. A review of light interception in plant stands from leaf to canopy in different plant functional types and in species with varying shade tolerance. *Ecological Research*, 25, 693–714.

Niklas, K.J., 1991. The elastic moduli and mechanics of *Populus tremuloides (Salicaceae)* petioles in bending and torsion. *American Journal of Botany*, 78, 989–996.

Nilsen, E.T., Forseth, I.N., 2018. The role of leaf movements for optimizing photosynthesis in relation to environmental variation. In: Adams III, W., Terashima, I. (Eds.) *The leaf: a platform for performing photosynthesis*. Cham: Springer International Publishing, pp. 401–423.

Nilson, T., 1971. A theoretical analysis of the frequency of gaps in plant stands. *Agricultural and Forest Meteorology*, 8, 25–38.

Nilson, T., 1999. Inversion of gap frequency data in forest stands. *Agricultural and Forest Meteorology*, 98–99 (0), 437–448.

Norman, J.M., Campbell, G.S., 1989. Canopy structure. In: Pearcy, R., Ehleringer, J., Mooney, H., Rundel, P. (Eds.). *Plant physiological ecology: Field methods and instrumentation*. Chapman and Hall, London, UK, pp. 301–325.

Oker-Blom, P., Kellomaki, S., Smolander, H., 1983. Photosynthesis of a Scots pine shoot: the effect of shoot inclination on the photosynthetic response of a shoot subjected to direct radiation. *Agricultural Meteorology*, 29, 191–206.

Ollinger, S.V., 2011. Sources of variability in canopy reflectance and the convergent properties of plants. *The New Phytologist*, 189, 375–394.

Pearcy, R.W., Yang, W., 1996. A three-dimensional crown architecture model for assessment of light capture and carbon gain by understory plants. *Oecologia*, 108, 1–12.

Pearcy, R.W., Valladares, F., Wright, S.J., de Paulis, E.L., 2004. A functional analysis of the crown architecture of tropical forest *Psychotria* species: do species vary in light capture efficiency and consequently in carbon gain and growth? *Oecologia*, 139, 163–177.

Pinty, B., Lavergne, T., Dickinson, R.E., Widlowski, J.-L., Gobron, N., Verstraete, M.M., 2006. Simplifying the interaction of land surfaces with radiation for relating remote sensing products to climate models. *Journal of Geophysical Research*, 111(D2), D02116.

Pisek, J., Ryu, Y., Alikas, K., 2011a. Estimating leaf inclination and G-function from leveled digital camera photography in broadleaf canopies. *Trees*, 25, 919–924.

Pisek, J., Lang, M., Nilson, T., Korhonen, L., Karu. H., 2011b. Comparison of methods for measuring gap size distribution and canopy non-randomness at Järvselja RAMI (Radiation transfer Model Intercomparison) test sites. *Agricultural and Forest Meteorology*, 151, 365–377.

Pisek, J., Oliphant, A.J., 2013. A note on the height variation of foliage clumping: comparison with remote sensing retrievals. *Remote Sensing Letters*, 4, 400–408.

Pisek, J., Sonnentag, O., Richardson, A.D., Mõttus, M., 2013a. Is the spherical leaf inclination angle distribution a valid assumption for temperate and boreal broad leaf tree species? *Agricultural and Forest Meteorology*, 169, 186–194.

Pisek, J., Ryu, Y., Sprintsin, M., He, L., Oliphant, A.J., Korhonen, L., Kuusk, J., Kuusk, A., Bergstrom, R., Verrelst, J., Alikas, K., 2013b. Retrieving vegetation clumping index from Multi-Angle Imaging Spectro-Radiometer (MISR) data at 275 m resolution. *Remote Sensing of Environment*, 138, 126–133.

Pisek, J., Govind, A., Arndt, S.K., Hocking, D., Wardlaw, T.J., Fang, H., Matteucci, G., Longdoz, B., 2015. Intercomparison of clumping index estimates from POLDER, MODIS and MISR satellite data over reference sites. *ISPRS Journal of Photogrammetry*, 101, 47–56.

Perry, G.L.W., Miller, B.P., Enright, N.J., 2006. A comparison of methods for the statistical analysis of spatial point patterns in plant ecology. *Plant Ecology*, 187 (1), 59–82.

Rasmussen, M.O., Göttsche, F.-M., Diop, D., Mbow, C., Olesen, F.-S., Fensholt, R., Sandholt, I., 2011. Tree survey and allometric models for tiger bush in northern Senegal and comparison with tree parameters derived from high resolution satellite data. *International Journal of Applied Earth Observation and Geoinformation*, 13 (4), 517–527.

Ross, J., 1975. Radiative transfer in plant communities. In: Monteith, J.L. (Ed.), *Vegetation and the Atmosphere*, vol. 1. Academic Press, London, UK, pp. 13–55.

Ross, J., 1981. *The Radiation Regime and Architecture of Plant Stands*. Junk Publishers, The Hague, pp. 391.

Roujean, J.L., Lacaze, R., 2002. Global mapping of vegetation parameters from POLER multiangular measurements for studies of surface-atmosphere interactions: a pragmatic method and its validation. *Journal of Geophysical Research*. 107 (D12), 4150.

Ryu, Y., Sonnentag, O., Nilson, T., Vargas, R., Kobayashi, H., Wenk, R., Baldocchi, D.D., 2010a. How to quantify tree leaf area index in a heterogeneous savanna ecosystem: a multi-instrument and multi-model approach. *Agricultural and Forest Meteorology*, 150, 63–76.

Ryu, Y., Nilson, T., Kobayashi, H., Sonnentag, O., Law, B.E., Balocchi, D.D., 2010b. On the correct estimation of effective leaf area index: does it reveal information on clumping effects. *Agricultural and Forest Meteorology*, 150, 463–472.

Sato, H., Itoh, A., Kohyama, T., 2007. SEIB-DGVM: a new dynamic global vegetation model using a spatially explicit individual-based approach. *Ecological Modelling*, 200, 279–307.

Sinoquet, H., Pincebourde, S., Adam, B., Dones, N., Phattaralerphong, J., Combes, D., Ploquin, S., Sangsing, K., Kasemsap, P., Thanisawanyangkura, S., Groussier-Bout, G., Casas, J., 2009. 3-D maps of tree canopy geometries at leaf scale. *Ecology*, 90, 283.

Smith, B., 2001. LPJ-GUESS – an ecosystem modelling framework. Department of Physical Geography and Ecosystems Analysis, INES, Sölvegatan, 12, 22362.

Stovall, A.E.L., Masters, B., Fatoyinbo, L., Yang, X., 2021. TLSLeAF: automatic leaf angle estimates from single-scan terrestrial laser scanning. *New Phytologist*, 232, 1876–1892.

Stroppiana, D., Boschetti, M., Confalonieri, R., Bocchi, S., Brivio, P.A., 2006. Evaluation of LAI-2000 for leaf area index monitoring in paddy rice. *Field Crops Research*, 99 (2–3), 167–170.

Tadrist, L., Saudreau, M., de Langre, E., 2014. Wind and gravity mechanical effects on leaf inclination angles, *Journal of Theoretical Biology*, 341, 9–16.

Utsugi, J., Araki, M., Kawasaki, R., Ishizuka, M., 2006. Vertical distributions of leaf area and inclination angle, and their relationship in a 46-year-old *Chamaecyparis obtusa* stand. *Forest Ecology and Management*, 225, 104–112.

Valladares, F, Guzman, B., 2006. Canopy structure and spatial heterogeneity of understory light in an abandoned Holm oak woodland. *Annals of Forest Science*, 63, 749–761.

Valladares, F., Niinemets, Ü., 2008. Shade tolerance, a key plant feature of complex nature and consequences. *Annual Review of Ecology, Evolution and Systematics*, 39, 237–257.

Walker, J., Tunstall, B.R., 1981. Field estimation of foliage cover in Australian woody vegetation. In: *Technical memorandum* 81/19. CSIRO, Canberra, p18.

Wang, Y.-P., Leuning, R., 1998. A two-leaf model for canopy conductance, photosynthesis and partitioning of available energy I: model description and comparison with a multi layered model. *Agricultural and Forest Meteorology*, 91, 89–111.

Wang, W.M., Li, Z.I., Su, H.B., 2007. Comparison of leaf angle distribution functions: effects on extinction coefficient and fraction of sunlit foliage. *Agricultural and Forest Meteorology*, 143, 106–122.

Warren Wilson, J., 1960. Inclined point quadrats. *New Phytologist*, 59, 1–7.

Wei, S., Fang, H., Schaaf, C.B., He, L., Chen, J.M., 2019. Global 500 m clumping index product derived from MODIS BRDF data (2001–2017). *Remote Sensing of Environment*, 232, 111296.

Welles, J.M., Norman, J.M., 1991. Instrument for indirect measurement of canopy architecture. *Agronomy Journal*, 83, 818–825.

Widlowski, J.L., Mio, C., Disney, M., Adams, J., Andredakis, I., Atzberger, C., Brennan, J., Busetto, L., Chelle, M., Ceccherini, G., Colombo, R,. Cote, J.-F., Eenmäe, A., Essery, R., Gastellu-Etchegorry, J.-P., Gobron, N., Grau, E., Haverd, V., Homolova, L., Huang, H., Hunt, L., Kobayashi, H., Koetz, B., Kuusk, A., Kuusk, J., Lang, M., Lewis, P.E., Lovell, J.L., Malenovsky, Z., Meroni, M., Morsdorf, F., Mõttus, M., Ni-Meister, W., Pinty, B., Rautiainen, M., Schlerf, M., Somers, B., Stuckens, J., Verstraete, M.M., Yang, W., Zhao, F., Zenone, T., 2015. The fourth phase of the radiative transfer model intercomparison (RAMI) exercise: actual canopy scenarios and conformity testing. *Remote Sensing of Environment*, 169, 418–437.

Woodgate, W., Armston, J.D., Disney, M., et al. 2017. Validating canopy clumping retrieval methods using hemispherical photography in a simulated Eucalypt forest. *Agricultural and Forest Meteorology*, 247, 181–193.

Wujeska-Klause, A., Crous, K.Y., Ghannoum, O., Ellsworth, D.S., 2019. Lower photorespiration in elevated CO_2 reduces leaf N concentrations in mature Eucalyptus trees in the field. *Global Change Biology*, 25, 1282–1295.

Yang, X., Li, R., Jablonski, A., Stovall. A., Kim, J., Yi, K., Ma, Y., Beverly, D., Phillips, R., Novick, K., Xu, X., Lerdau, M., 2023. Leaf angle as a leaf and canopy trait: Rejuvenating its role in ecology with new technology. *Ecology Letters*, 26, 1005–1020.

Yin, H.C., 1938. Diaphototropic movement of the leaves of Malva neglecta. *American Journal of Botany*, 25 (1), 1–6.

Zou, J., Yan, G., Chen, L., 2015. Estimation of Canopy and Woody Components Clumping Indices at Three Mature *Picea crassifolia* Forest Stands. *IEEE Journal of Selected Topics in Applied Earth Observations and Remote Sensing,* 8(4), 1413–1422.

SUMMARY IN ESTONIAN

Digifotograafia rakendatavus lehenurkade ja klasteriseerumisindeksi muutuste jälgimisel

Valgusel on ülioluline roll puuvõrades toimuvates protsessides, mõjutades fotosünteesi intensiivsust, taimede kasvu ja primaarproduktsiooni. See, mil määral valgus võra sisse jõuab, sõltub muuhulgas oluliselt lehtede kaldenurkadest ning klasteriseerumisindeksist, mis kirjeldab lehtede grupeerumist võrsetesse, okstesse ja teistesse struktuuridesse. Mõlemad parameetrid on hädavajalikud nii taimkatte produktiivsuse kui ka kiirguslevi modelleerimisel, ent tulenevalt nende mõõtmise keerukusest ja töömahukusest on neid mudelites sageli käsitletud konstantidena või hoopis eiratud.

Käesolevas väitekirjas võeti eesmärgiks uurida nii lehenurki kui klasteriseerumisindeksit digifotograafial põhinevate meetoditega. Digifotodelt lehenurkade mõõtmine on suhteliselt lihtne ja kättesaadav meetod, ning töös näidati, et selle kasutamiseks ei ole vaja erilisi eelteadmisi või oskusi, oluline on vaid tähelepanelikkus. Lehenurkade muutlikkuse kirjeldamiseks mõõdeti lehenurki levinud lehtpuudel mitmel erineval kõrgusel kogu vegetatsiooniperioodi jooksul. Selgus, et lehenurkade jaotus varieerub märkimisväärselt sõltuvalt puuliigist, kõrgusest võras, kasvuperioodi etapist ja valguse kättesaadavusest. Suurim ajaline muutlikkus ilmnes kasvuperioodi alguses ja lõpus, samas kui ülejäänud kasvuperioodi vältel püsisid lehenurkade jaotused suhteliselt stabiilsed. Kõige tugevam muutlikkus ilmnes puulatvades, vähenedes võras madalamale liikudes. Valgustatus mõjutas enim vertikaalsemaid, järsu nurga all kasvavaid puulehti, samas kui horisontaalsete lehtedega liikide lehenurkade jaotused püsisid stabiilsed sõltumata kasvukohast ja ligi pääsevast valgusest.

Klasteriseerumisindeksi puhul võrreldi nelja erinevat andmekogumis- ja kuut arvutusmeetodit kahes erinevas metsas kahel eri perioodil aastas. Leiti, et ka siin annavad häid tulemusi digifotograafial põhinevad andmekogumisviisid, eelkõige digitaalsed poolsfäärifotod. Rakendades poolsfäärifotodelt saadud andmetele arvutusmeetodeid, mis põhinevad logaritmilisel keskmisel kombineerituna avade suurusjaotusega, saadi tulemused, mis kirjeldasid võraelementide grupeerumist kõige tugevamana. Alternatiivsete meetoditega arvutatud klasteriseerumisindeksi väärtused viitasid juhuslikumalt struktureeritud võrale ning esindavad minimaalset klasteriseerumist, mida peaks igal juhul arvesse võtma.

Töö käigus koguti kõige suurem ja mitmekesisem teadaolev lehenurgaandmestik, mis hõlmab üle kahesaja liigi kolmelt mandrilt, ning tehti see laiemale kogukonnale avalikult kättesaadavaks. Ühtlasi uuriti, kuidas mõjutab nende andmete kasutatavust kliimamuutustega kaasnev kõrgem CO_2 kontsentratsioon atmosfääris. Ilmnes, et CO_2 kontsentratsioonil puudub märkimisväärne mõju nii klasteriseerumisindeksile kui lehenurkadele, mistõttu jääb kogutud andmehulk kasulikuks ka tulevikus.

ACKNOWLEDGEMENTS

I would like to express my deepest gratitude to my supervisor, Jan Pisek, for his invaluable guidance, enduring patience, and encouragement throughout this thesis. This work would not have been possible without his support. I am also thankful to the vegetation remote sensing group in Tartu Observatory, particularly Tiit Nilson and Mait Lang, for their support and valuable discussions. I extend my thanks to all the coauthors of the research papers included in this thesis for their contribution and advice.

I acknowledge the funding provided by the Estonian Science Foundation grants no. PUT232, PUT1355, and PRG1405 which made this research possible. I am also grateful to the Kristjan Jaak scholarship program, Tartu College in Toronto and prof. Jing M. Chen at the University of Toronto for the opportunities to broaden my academic horizon.

Finally, my heartfelt thanks go to my family and friends. I thank my parents, Kaja and Rein, for their unwavering support, my husband Aiko for always helping me maintain perspective, my children Anett, Artur and Aksel for their joy and curiosity, and my dearest friends Kristiina, Maris and Kärt for their ever-present optimism and encouragement throughout this journey. Special thanks to Maris and Tauri for the best company during conferences and seminars, as well as Alina, Indrek, Joosep and Tõnu for the much-needed laughs.

PUBLICATIONS

CURRICULUM VITAE

Name: Kairi Adamson (née Raabe)
Date of birth: 01.05.1990
Nationality: Estonian
E-mail: adamson.kairi@gmail.com

Education:

2014–…	University of Tartu, Tartu Observatory, Environmental Technology (PhD studies)
2012–2014	University of Tartu, Environmental Technology (MSc, *cum laude*)
2009–2012	University of Tartu, Environmental Technology (BSc)

Professional employment:

07.2018–…	Analyst, Cybernetica OÜ
01.2018–08.2018	Junior Research Fellow, University of Tartu, Tartu Observatory
04.2017–07.2018	System Analyst, Turnit OÜ
09.2014–12.2017	Junior Researcher, Tartu Observatory
03.2014–05.2014	Technician, Tartu Observatory
05.2009–05.2014	Translator, Kirjastus Pegasus OÜ

Awards:

2013	Juhan Ross scholarship

Publications:

Pisek, J., Reznickova, L., **Adamson, K.**, Ellsworth, D.S. (2021) Leaf inclination angle and foliage clumping in an evergreen broadleaf Eucalyptus forest under elevated atmospheric CO_2. Australian Journal of Botany, 69(8), 622–629.

Pisek, J., **Adamson, K.** (2020) Dataset of leaf inclination angles for 71 different Eucalyptus species. Data in Brief, 33.

Kattge, J., Boenisch, G., Diaz, S., Lavroel, S., Prentice, I.C., Leadley, P., Tautenhahn, S., Werner, G., …, **Adamson, K.**, et al. (2020) TRY plant trait database – enhanced coverage and open access. Global Change Biology, 26 (1), 119–188.

Meerdink, S., Roberts, D., Hulley, G., Gader, P., Pisek, J., **Adamson, K.**, King, J., Hook, S.J. (2019) Plant species' spectral emissivity and temperature using the hyperspectral thermal emission spectrometer (HyTES) sensor. Remote Sensing of Environment, 224, 421–435.

Chianucci, F., Pisek, J., **Raabe, K.**, Marchino, L., Ferrara, C., Corona, P. (2018) A dataset of leaf inclination angles for temperate and boreal broadleaf woody species. Annals of Forest Science, 75, 50.

Raabe, K., Pisek, J., Lang, M., Korhonen, L. (2017) Estimating the beyond-shoot foliage clumping at two contrasting points in the growing season using a variety of field-based methods. Trees – Structure and Function, 31(4), 1–7.

Pisek, J., Chen, J.M., Kobayashi, H., Rautiainen, M., Schaepman, M.E., Karnieli, A., Sprintsin, M., Ryu, Y., Nikopensius, M., **Raabe, K.** (2016) Retrieval of seasonal dynamics of forest understory reflectance from semiarid to boreal forests using MODIS BRDF data. Journal of Geophysical Research Biogeosciences, 121(3), 1–9.

Nikopensius, M., Pisek, J., **Raabe, K.** (2015) Spectral reflectance patterns and seasonal dynamics of common understory types in three mature hemi-boreal forests. International Journal of Applied Earth Observation and Geoinformation, 43, 84–91.

Raabe, K., Pisek, J., Sonnentag, O., Annuk, K. (2015) Variations of leaf inclination angle distribution with height over the growing season and light exposure for eight broadleaf tree species. Agricultural and Forest Meteorology, 214–215, 2–11.

Pisek, J., Rautiainen, M., Nikopensius, M., **Raabe, K.** (2015) Estimation of seasonal dynamics of understory NDVI in northern forests using MODIS BRDF data: Semi-empirical versus physically-based approach. Remote Sensing of Environment, 163, 42–47.

ELULOOKIRJELDUS

Nimi:	Kairi Adamson (sünd. Raabe)
Sünniaeg:	01.05.1990
Rahvus:	eesti
E-mail:	adamson.kairi@gmail.com

Haridus:

2014–…	Tartu Ülikool, Tartu Observatoorium, keskkonnatehnoloogia (doktoriõpe)
2012–2014	Tartu Ülikool, keskkonnatehnoloogia (MSc, *cum laude*)
2009–2012	Tartu Ülikool, keskkonnatehnoloogia (BSc)

Teenistuskäik:

07.2018–…	analüütik, Cybernetica OÜ
01.2018–08.2018	nooremteadur, Tartu Ülikool, Tartu Observatoorium
04.2017–07.2018	süsteemianalüütik, Turnit OÜ
09.2014–12.2017	nooremteadur, Tartu Observatoorium
03.2014–05.2014	tehnik, Tartu Observatoorium
05.2009–05.2014	tõlkija, Kirjastus Pegasus OÜ

Teaduspreemiad:

2013	Juhan Rossi nimeline stipendium

Publikatsioonid:

Pisek, J., Reznickova, L., **Adamson, K.**, Ellsworth, D.S. (2021) Leaf inclination angle and foliage clumping in an evergreen broadleaf Eucalyptus forest under elevated atmospheric CO_2. Australian Journal of Botany, 69(8), 622–629.

Pisek, J., **Adamson, K.** (2020) Dataset of leaf inclination angles for 71 different Eucalyptus species. Data in Brief, 33.

Kattge, J., Boenisch, G., Diaz, S., Lavroel, S., Prentice, I.C., Leadley, P., Tautenhahn, S., Werner, G., …, **Adamson, K.**, et al. (2020) TRY plant trait database – enhanced coverage and open access. Global Change Biology, 26 (1), 119–188.

Meerdink, S., Roberts, D., Hulley, G., Gader, P., Pisek, J., **Adamson, K.**, King, J., Hook, S.J. (2019) Plant species' spectral emissivity and temperature using the hyperspectral thermal emission spectrometer (HyTES) sensor. Remote Sensing of Environment, 224, 421–435.

Chianucci, F., Pisek, J., **Raabe, K.**, Marchino, L., Ferrara, C., Corona, P. (2018) A dataset of leaf inclination angles for temperate and boreal broadleaf woody species. Annals of Forest Science, 75, 50.

Raabe, K., Pisek, J., Lang, M., Korhonen, L. (2017) Estimating the beyond-shoot foliage clumping at two contrasting points in the growing season using a variety of field-based methods. Trees – Structure and Function, 31(4), 1–7.

Pisek, J., Chen, J.M., Kobayashi, H., Rautiainen, M., Schaepman, M.E., Karnieli, A., Sprintsin, M., Ryu, Y., Nikopensius, M., **Raabe, K.** (2016) Retrieval of seasonal dynamics of forest understory reflectance from semiarid to boreal forests using MODIS BRDF data. Journal of Geophysical Research Biogeosciences, 121(3), 1–9.

Nikopensius, M., Pisek, J., **Raabe, K.** (2015) Spectral reflectance patterns and seasonal dynamics of common understory types in three mature hemi-boreal forests. International Journal of Applied Earth Observation and Geoinformation, 43, 84–91.

Raabe, K., Pisek, J., Sonnentag, O., Annuk, K. (2015) Variations of leaf inclination angle distribution with height over the growing season and light exposure for eight broadleaf tree species. Agricultural and Forest Meteorology, 214–215, 2–11.

Pisek, J., Rautiainen, M., Nikopensius, M., **Raabe, K.** (2015) Estimation of seasonal dynamics of understory NDVI in northern forests using MODIS BRDF data: Semi-empirical versus physically-based approach. Remote Sensing of Environment, 163, 42–47.

DISSERTATIONES TECHNOLOGIAE CIRCUMIECTORUM UNIVERSITATIS TARTUENSIS

1. **Sille Teiter**. Emission rates of N_2O, N_2, CH_4 and CO_2 in riparian grey alder forests and subsurface flow constructed wetlands. Tartu, 2005, 134 p.
2. **Kaspar Nurk**. Relationships between microbial characteristics and environmental conditions in a horizontal subsurface flow constructed wetland for wastewater treatment. Tartu, 2005, 123 p.
3. **Märt Öövel**. Performance of wastewater treatment wetlands in Estonia. Tartu, 2006, 148 p.
   Sergei Yurchenko. Determination of some carcinogenic contaminants in food. Tartu, 2006, 143 p. Published in *Dissertation Chimicae Universitatis Tartuensis,* 51.
4. **Alar Noorvee**. The applicability of hybrid subsurface flow constructed wetland systems with re-circulation for wastewater treatment in cold climates. Tartu, 2007, 117 p.
   Ülle Jõgar. Conservation and restoration of semi-natural floodplain meadows and their rare plant species. Tartu, 2008, 99 p. Published in *Dissertation Biologicae Universitatis Tartuensis*, 139.
5. **Christina Vohla**. Phosphorus removal by various filter materials in subsurface flow constructed wetlands. Tartu, 2008, 103 p.
6. **Martin Maddison**. Dynamics of phytomass production and nutrient standing stock of cattail and its use for environment-friendly construction. Tartu, 2008, 87 p.
7. **Marika Truu**. Impact of land use on microbial communities in Estonian soils. Tartu, 2008, 126 p.
8. **Elar Põldvere**. Removal of organic material, nitrogen and phosphorus from wastewater in hybrid subsurface flow constructed wetlands. Tartu, 2009, 107 p.
9. **Margit Kõiv**. Treatment of landfill leachate and municipal wastewater in subsurface flow filters using mineralized peat and hydrated oil shale ash. Tartu, 2010, 147 p.
10. **Jaanis Juhanson**. Impact of phytoremediation and bioaugmentation on the microbial community in oil shale chemical industry solid waste. Tartu, 2010, 95 p.
    Aare Selberg. Evaluation of environmental quality in Northern Estonia by the analysis of leachate. Tartu, 2010, 117 p. Published in *Dissertation Chimicae Universitatis Tartuensis,* 99.
11. **Riho Mõtlep**. Composition and diagenesis of oil shale industrial solid wastes. Tartu, 2010, 127 p.
12. **Igor Zaytsev**. Bioaugmentation in LWA-filled horizontal subsurface flow filters for wastewater treatment: Impact of flow regime, temperature and donor system Tartu, 2010, 97 p.

13. **Siiri Velling**. Microbial BOD biosensor for wastewater analysis. Tartu, 2011, 79 p.
14. **Riina Lepik**. Biodegradability of phenolic compoundsas single and mixed substrates by activated sludge. Tartu, 2011, 153 p.
15. **Liis Marmor**. Ecology and bioindicative value of epiphytic lichens in relation to air pollution and forest continuity. Tartu, 2011, 98 p.
16. **Martin Liira**. Active filtration of phosphorus in Ca-rich hydrated oil shale ash: precipitation mechanisms and recovery. Tartu, 2012, 84 p.
17. **Kristjan Karabelnik**. Advanced design and management of hybrid constructed wetlands: environmental and water purification effects. Tartu, 2012, 128 p.
18. **Hiie Nõlvak**. Influence of qPCR workflow on target gene enumeration from environmental samples in the case of bioremediation potential estimation. Tartu, 2012, 136 p.
19. **Merlin Raud**. Study of semi-specific BOD biosensors for biosensor-array. Tartu, 2013, 103 p.
20. **Ivar Zekker**. Enrichment of anaerobic ammonium oxidizing bacteria for nitrogen removal from digester effluent and anammox process acceleration by intermediate compounds. Tartu, 2013, 142 p.
21. **Annika Uibopuu**. Communities of arbuscular mycorrhizal fungi in spruce forest ecosystem and their effect on performance of forest understorey plant species. Tartu, 2013, 104 p.
22. **Jekaterina Jefimova**. Leaching of polycyclic aromatic hydrocarbons (PAHs) and heavy metals from the oil shale processing wastes and from waste-based products. Tartu, 2015, 184 p.
23. **Teele Ligi**. Bacterial community structure and its genetic potential for nitrogen removal in the soils and sediments of a created riverine wetland complex. Tartu, 2015, 127 p.
24. **Kuno Kasak**. Greenhouse gas emissions and water treatment efficiency in subsurface flow filters using various substrates. Tartu, 2016, 128 p.
25. **Martin Ligi**. Application of close range remote sensing for monitoring aquatic environment. Tartu, 2017, 146 p.
26. **Mikk Espenberg**. Impact of management on peatland microbiome and greenhouse gas emissions. Tartu, 2017, 152 p.
27. **Jens-Konrad Preem**. Forest soil bacterial community analysis using high-throughput amplicon sequencing. Tartu, 2017, 108 p.
28. **Taavi Vaasma**. Enrichment, atmospheric dispersion and deposition of naturally occurring radionuclides from oil shale-fired power plants. Tartu, 2017, 175 p.
29. **Kristjan Oopkaup**. Microbial community and its relationship with pollutant removal in treatment wetlands. Tartu, 2018, 154 p.
30. **Ergo Rikmann**. Autotrophic nitrogen removal and relevant equilibrial processes. Tartu, 2019, 179 p.
31. **Kati Klein**. Studies and treatment of inhibitory and recalcitrant wastewater. Tartu, 2021, 168 p.

32. **Thomas Schindler**. Tree stem CH_4 and N_2O fluxes in various forest ecosystems. Tartu, 2021, 182 p.
33. **Peeter Paaver**. Development of alternative binders based on oil shale fly ash. Tartu, 2021, 130 p.
34. **Kertu Tiirik**. Antibiotic resistance in connected engineered and natural aquatic environments. Tartu, 2021, 124 p.
35. **Keit Kill**. Nutrient fluxes regulation in an in-stream constructed wetland treating polluted agricultural runoff. Tartu, 2022, 144 p.
36. **Rauno Lust**. Bioelectrochemical systems for enhanced removal of nitrate from water with a low electron donor concentration. Tartu, 2022, 145 p.
37. **Mihhail Fetissov**. Spatial decision support systems for ecosystem-based marine management. Tartu, 2022, 172 p.
38. **Mohit Masta**. Isotopologue and microbiome studies for N_2O source attribution in peat soils. Tartu, 2022, 113 p.
39. **Mirjam Uusõue**. Suspended particles dynamics and characteristics in optically complex waterbodies. Tartu, 2023, 144 p.
40. **Sharvari Sunil Gadegaonkar**. Microbial and environmental factors affecting the nitrate removal efficiency from water in bioelectrochemical systems. Tartu, 2023, 124 p.
41. **Kalev Uiga**. Modelling and experimental measurement of the closed equilibrium systems of $CaS–H_2O$ and $SrS–H_2O$. Tartu, 2023, 137 p.
42. **Ave Ansper-Toomsalu**. Synergy of Earth Observation data to advance monitoring of optically complex waters. Tartu, 2024, 256 p.